SAN FRANCISCO ESTUARY & WATERSHED SCIENCE
Sponsored by the Delta Stewardship Council and UC Davis Institute of the Environment

RESEARCH

Spatial and Temporal Patterns of Cyanobacterial Harmful Algal Blooms in the Sacramento–San Joaquin Delta: Implications for Monitoring and Research

Ellen P. Preece[1]*, Gry Mine Berg[2], Karen Odkins[3], Tricia Lee[4], Timothy G. Otten[5]

ABSTRACT

Cyanobacteria harmful algal bloom (CHAB) events, often dominated by the cyanobacteria genus *Microcystis*, are a major water-quality issue in the large, hydrologically complex, Sacramento–San Joaquin Delta (Delta). To improve future CHAB-specific monitoring, we analyzed historical data to characterize spatial and habitat-based patterns in CHAB occurrence. We identified three primary habitat types that support CHABs to various degrees: (1) dead-end channels and marinas, which tend to support the highest densities and most frequent blooms; (2) flooded islands, shallow side channels, and sloughs, where CHABs occur less frequently, and generally at lower densities, and (3) main channels, where CHABs occur but typically at lower intensities and without the surface accumulations observed in dead-end channels. Data from routine monitoring programs and special studies were used to evaluate CHAB variation across Delta regions and among these habitat types. Monitoring metrics included chlorophyll-*a* (chl-*a*), *Microcystis* abundance determined by microscopy and quantitative polymerase chain reaction (qPCR), microcystin toxin concentrations, and *Microcystis* Visual Index (MVI) scores. July through October was identified as peak CHAB season, with CHAB severity greatest in the South Delta, Central Delta, and San Joaquin River regions. CHABs and associated toxins were infrequent in the Sacramento River, Cache Slough Complex, and East Delta regions, with microcystin concentrations typically below detection (0.15 µg L^{-1}) and always below the California health-based warning trigger of 6.0 µg L^{-1}. Dead-end channel habitats exhibited significantly higher microcystin concentrations than other habitat types, with nearly 40% of samples exceeding the California caution trigger of 0.8 µg L^{-1}, compared to 10% in flooded islands and 7% in main channels. Based on these findings, we recommend enhanced sampling in dead-end channels and continued CHAB monitoring to identify and refine risk forecasts under changing climate conditions.

SFEWS Volume 24 | Issue 3 | Article 3

https://doi.org/10.15447/sfews.2026v24iss3art3

* Corresponding author: *ellen.preece@water.ca.gov*

1 California Department of Water Resources
West Sacramento, CA 95691 USA

2 Coastal Conservation and Research
Moss Landing, CA 95039 USA

3 California Department of Fish and Wildlife
West Sacramento, CA 95605 USA

4 *Current:* California Stormwater Quality Association
Redondo Beach, CA 90277 USA
Former: Delta Stewardship Council
Delta Science Program
Sacramento, CA 95814 USA

5 Bend Genetics
Sacramento, CA 95825 USA

INTRODUCTION

Like many water bodies worldwide (Harke et al. 2016), the Sacramento–San Joaquin Delta (Delta) experiences annual cyanobacteria harmful algal bloom (CHAB) events (Lehman et al. 2017). Toxins produced by cyanobacteria (cyanotoxins) can lead to a wide range of harmful effects, including mortality in aquatic animals, waterfowl, and domestic animals (Havens 2008; Miller et al. 2010). When present in drinking-water supplies, cyanotoxins can pose adverse health risks and often necessitate costly treatment to be removed (Cheung et al. 2013). CHABs can also affect local economies and lead to revenue losses by reducing business in affected water bodies during the peak of tourism season. Considerable costs are associated with mitigation of CHABs (Dodds et al. 2009). These effects are of particular concern in the Delta, which serves as a critical source of drinking water for millions of Californians, supports extensive recreational use, and provides habitat for threatened and endangered species.

Delta CHAB events are typically dominated by the genus *Microcystis*, which can produce toxins (Lehman et al. 2017, 2022). Other common cyanobacteria which have also been observed in some portions of the Delta include genera such as *Aphanizomenon*, *Planktothrix, Dolichospermum*, *Pseudanabaena*, and *Planktolyngbya* (Lehman et al. 2008; Spier et al. 2013; Lehman et al. 2017, 2022; Perry et al. 2023). Because *Microcystis* is the primary bloom-forming and toxin-producing genus in the Delta, it is the focus of this paper.

Although several programs collect water-quality data relevant to CHABs across the Delta, there is currently no dedicated, routine CHAB monitoring program. An effective dedicated CHAB program would collect the necessary data types at appropriate temporal and spatial frequencies to characterize trends, identify areas of greatest concern, and ultimately predict bloom events. In practice, this is very challenging since many environmental parameters are involved in cyanobacteria growth, and there are high temporal and spatial variability in CHAB biomass and community composition (Howard et al. 2023). These challenges are compounded by the Delta's complex hydrology, expansive size, and reticulate configuration, all of which limit the ability to draw conclusions on broader spatial or temporal scales and complicate the inference of CHAB patterns (Jassby et al. 1995; Kimmerer 2004).

The Delta CHAB Strategy was published in late 2024 (Preece, Berg, et al. 2024) to begin addressing the many CHAB monitoring challenges in the Delta. Key objectives included coordinating priority data collection, fostering collaborative data sharing, and identifying effective mitigation measures, while aligning scientific expertise with community engagement to improve understanding and management of CHABs. This is the second of two papers that build upon the work presented in the Delta CHAB Strategy. In the first paper, we synthesized existing environmental data—including water temperature, salinity, turbidity, and nutrients—derived from several different Delta water-quality monitoring programs (Preece et al., this issue). Here, we extend that work by further synthesizing available data to examine spatial variation in CHAB occurrence across the Delta. First, we define the different habitat types in the Delta that are known to support CHABs. We then use available datasets to identify parameters for quantifying CHABs, synthesize these data to identify areas most prone to CHABs, and then analyze temporal and regional CHAB patterns across the Delta. Collectively, the information presented in the first paper, together with the findings of this paper, can be used to inform strategies to incorporate into future Delta monitoring efforts.

HABITAT TYPES THAT INFLUENCE CYANOBACTERIA BLOOM DYNAMICS IN THE DELTA

Three primary habitat types found in the Delta support CHABs to varying degrees (Figure 1): (1) dead-end channels and marinas, (2) flooded islands and shallow side channels, and (3) main channels. While conditions within each habitat type can vary, this classification focuses on the physical parameters most relevant to *Microcystis* growth in the Delta, including flow, water depth, temperature, and irradiance which

differ across these habitat types (Lehman et al. 2017). This broad classification helps illustrate how CHABs differ across the Delta, though site-specific conditions also play an important role in their development, and these classifications cannot capture all local variations. Even so, distinguishing these habitat types offers valuable insight into why some environments favor CHAB formation more than others.

Areas with the densest *Microcystis* CHABs and highest cyanotoxin concentrations are in dead-end channels and marinas such as Discovery Bay and the Stockton Waterfront (Preece, Berg, et al. 2024). Similar observations of dense *Microcystis* have also been observed in other dead-end channels and marinas across the Delta such as Tiki Lagoon, Buckley Cove, and Windmill Cove (Preece et al. 2025). These areas are characterized by warmer temperatures, less flushing, weaker vertical mixing, lower degree of sediment re-suspension, and longer residence times, leading to less dilution and greater accumulation of CHAB cells than in mainstem channels or flooded islands (Figure 1). Because the water column is relatively clear in this type of environment, the euphotic zone depth (Z_e) to total mixed water depth (Z_m)—i.e., the Z_e:Z_m ratio—may be high enough that CHAB cells spend a greater time in the euphotic zone, leading to higher primary productivity compared with the main channel environment (Figure 1). The euphotic zone in these areas may reach the sediment–water interface, and *Microcystis* may become denser and more evenly distributed throughout the water column.

Microcystis is known to thrive in high light, likely in part because of its large, colonial morphology, which helps alleviate UV stress by self-shading (Xiao et al. 2018). In a relatively calm water column, the large colonies also enable high vertical velocity (buoyancy), which allows the cells to maintain a position at the surface. By maintaining their position near the surface, dense blooms may shade out non-buoyant phytoplankton competitors (Humphries and Lyne 1988; Reynolds 1994). In addition to calm water and greater water clarity, dead-end sloughs and marinas typically experience less flushing and longer residence times, which can result in a stronger coupling with the sediments, aiding the exchange of materials, including overwintering cyanobacteria cells and nutrients (Zhu et al. 2021).

The second habitat type known to support CHABs are the areas identified as flooded islands, shallow side channels, and sloughs (Lehman et al. 2015). While this habitat type spans a range of geographic locations and hydrodynamic conditions across the Delta, these areas share shallower depths than the main channels, greater Ze:Zm ratios, and intermediate flushing rates relative to both dead-end channels and main channels. Flooded-island areas function as large tidal lakes with several outlets that allow exchange with the broader Delta. Two of the most well-studied flooded islands are Mildred Island and Franks Tract (e.g., Lucas et al. 2002; Lopez et al. 2006). Side channels and sloughs are grouped with flooded islands because they share similar hydrodynamic influences, such as flow rate, lateral advection, and tidal forcings, but are generally shallower than flooded islands with Z_e:Z_m ratios that approach or exceed 1 (i.e., the euphotic zone reaches the sediments). These shallower depths may support greater phytoplankton productivity, including productivity of CHAB species, relative to main channel sites (Figure 1B, 1C). At the same time, relatively shallow depths increase sediment contact, exposing phytoplankton to filter-feeding bivalves and to competition with submerged aquatic vegetation (SAVs) for nutrients and light. Grazing by filter-feeders could limit CHAB biomass if CHAB species were consumed at rates comparable to other phytoplankton genera, while SAV competition may further constrain nutrient availability (Lucas et al. 2002, 2006).

Although flooded islands tend to be relatively shallow and have a greater Z_e:Z_m ratio than main channels, unlike dead-end sloughs and marinas they are distinguished by higher stream flow, tidal forcing, and flushing rates. These relatively high flushing rates—and resulting low residence times—act as negative drivers of CHAB

https://doi.org/10.15447/sfews.2026v24iss3art?

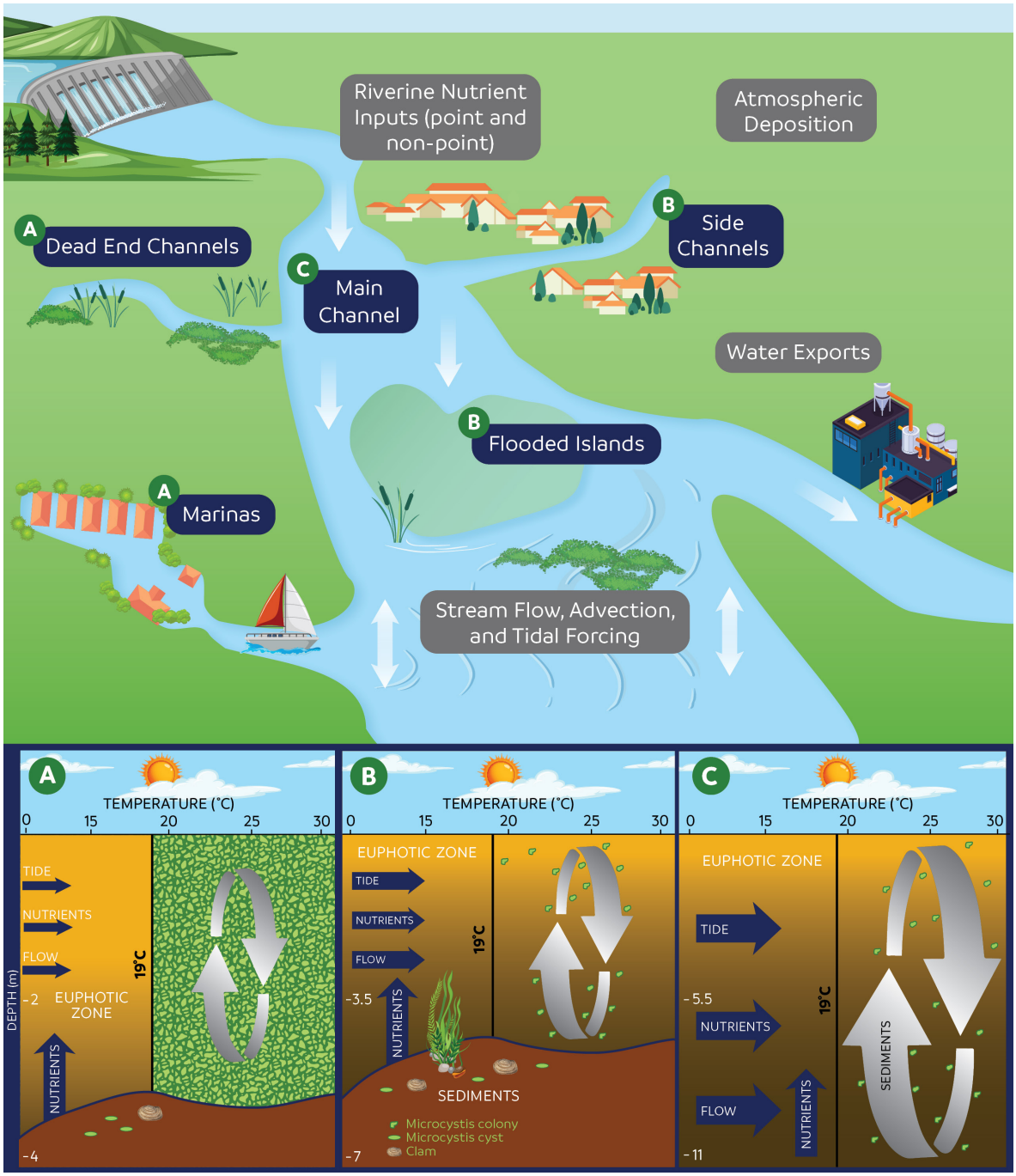

Figure 1 *Top panel*: Different physical environments provided by Delta waterways that influence CHAB development, including (**A**) dead-end channels and marinas, (**B**) flooded islands, side channels, and small sloughs with submerged aquatic vegetation (SAV), and (**C**) main channels. Processes that interact with these different types of physical environments include input of point and non-point nutrient sources, stream flow and tidal forcing, water exports, and atmospheric deposition. *Bottom panels*: Representations of water column characteristics of (**A**) dead-end channels and marinas, (**B**) flooded islands, side channels, and small sloughs and (**C**) main channels. In the *bottom panels*, depth (m) is shown on the *y*-axis and temperature (°C) on the *x*-axis. The 19 °C threshold indicated in each panel represents the minimum water temperature associated with *Microcystis* bloom initiation in the Delta (Lehman et al. 2013). The thickness of the *blue arrows* represents the relative influence of tide, nutrients, and flow within each habitat type. In panel **A**, the entire water column falls within the euphotic zone, as indicated by the dense *Microcystis* colony distribution throughout, in contrast to panels **B** and **C** where the euphotic zone is limited to the uppermost portion of the water column. The *large grey curved arrows* represent vertical mixing intensity, with the sediments label in panel **C** indicating that strong vertical mixing in main channels results in active re-suspension of sediments.

development and occurrence compared with typical dead-end channels and sloughs.

In comparison with flooded islands, main channels are characterized as having stronger stream flow, higher rate of flushing, tidal forcing, continuous vertical mixing, and a high degree of sediment re-suspension (Lucas et al. 2002; Kimmerer et al. 2019). Main channels also tend to have a deeper water column than flooded islands. In this environment, CHAB species such as *Microcystis* are mixed throughout the water column and spend limited time in the euphotic zone because the Z_e:Z_m ratio may be 0.5 or less (Figure 1C). In addition to vertical mixing, colony densities may also be limited by relatively short residence times and dilution. Both limited time in the euphotic zone and vigorous physical mixing may produce lower growth rates (Lehman et al. 2008) as well as decreasing the ability of cells to aggregate and accumulate.

STUDY DESIGN AND METHODS

Phytoplankton biomass, including biomass of CHAB genera, is typically measured as the concentration of the light-harvesting pigment chlorophyll-*a* (chl-*a*). This biomass measurement includes the whole phytoplankton community and does not indicate the fractional contribution of different species. Nevertheless, chl-*a* serves as a key biological indicator of algal biomass and trophic status, providing an early warning of eutrophication and CHABs (Gupta and Gupta 2025). Thus, it is a useful parameter for monitoring CHABs when interpreted alongside other cyanobacteria-specific indicators. Measurements used to indicate the individual contributions of species to community composition and biomass include cell abundance, cell biovolumes, and copy numbers of species-specific genes. In addition to the above-mentioned biomass indicators, ranges of parameters that generally vary with CHAB biomass—such as cyanotoxin concentrations and seedstock—can also be measured. In this paper we define CHAB parameters as the analytes and techniques commonly utilized to investigate CHABs in the Delta. Our analyses focus on phytoplankton biomass measurements, including chl-*a*, *Microcystis* units analyzed microscopically, *Microcystis* analyzed by quantitative polymerase chain reaction (qPCR), cyanotoxins, overwintering *Microcystis* seedstock, and the MVI data.

Geographic Regions

To facilitate our analysis of CHAB occurrences, the Delta was divided into eight geographic regions; the Cache Slough Complex (CSC), the upper Sacramento River (USR); the lower Sacramento River (LSR); the Central Delta (CD); the lower San Joaquin River (LSJR); the upper San Joaquin River (USJR); the South Delta (SD); and the East Delta (ED) (Figure 2). These regions were delineated based on known information about Delta CHABs and previous studies that have divided the Delta into regions for ecological comparisons (Bouma–Gregson et al. 2024; Hartman et al. 2024). Within three of these regions (the LSJR, CD, and USJR) cyanotoxin data were available for three known CHAB hotspots: Big Break, Discovery Bay, and the Stockton Waterfront—as well as limited data from other dead-end areas including Buckley Cove and Windmill Cove. Data from these hotspots were analyzed separately from the rest of the regional data. Alongside regional patterns, where data permit, the analyses also considered the three habitat types discussed above; dead-end channels and marinas, flooded islands/side channels/small sloughs, and main channel environments.

Data

A few ongoing monitoring efforts collect water-quality data related to CHABs that are available from public data portals (Table 1). Although these monitoring programs are not in place specifically for CHABs, they collect useful data relevant to understanding CHABs across the Delta. Agencies that manage water-quality monitoring stations include the California Department of Water Resources (CDWR), California Department of Fish and Wildlife (CDFW), United States Bureau of Reclamation (USBR Reclamation), and the US Geological Survey (USGS). In the following sections we synthesize data from these programs that were consolidated from the California Data Exchange Center (CDEC) and the

https://doi.org/10.15447/sfews.2026v24iss3art?

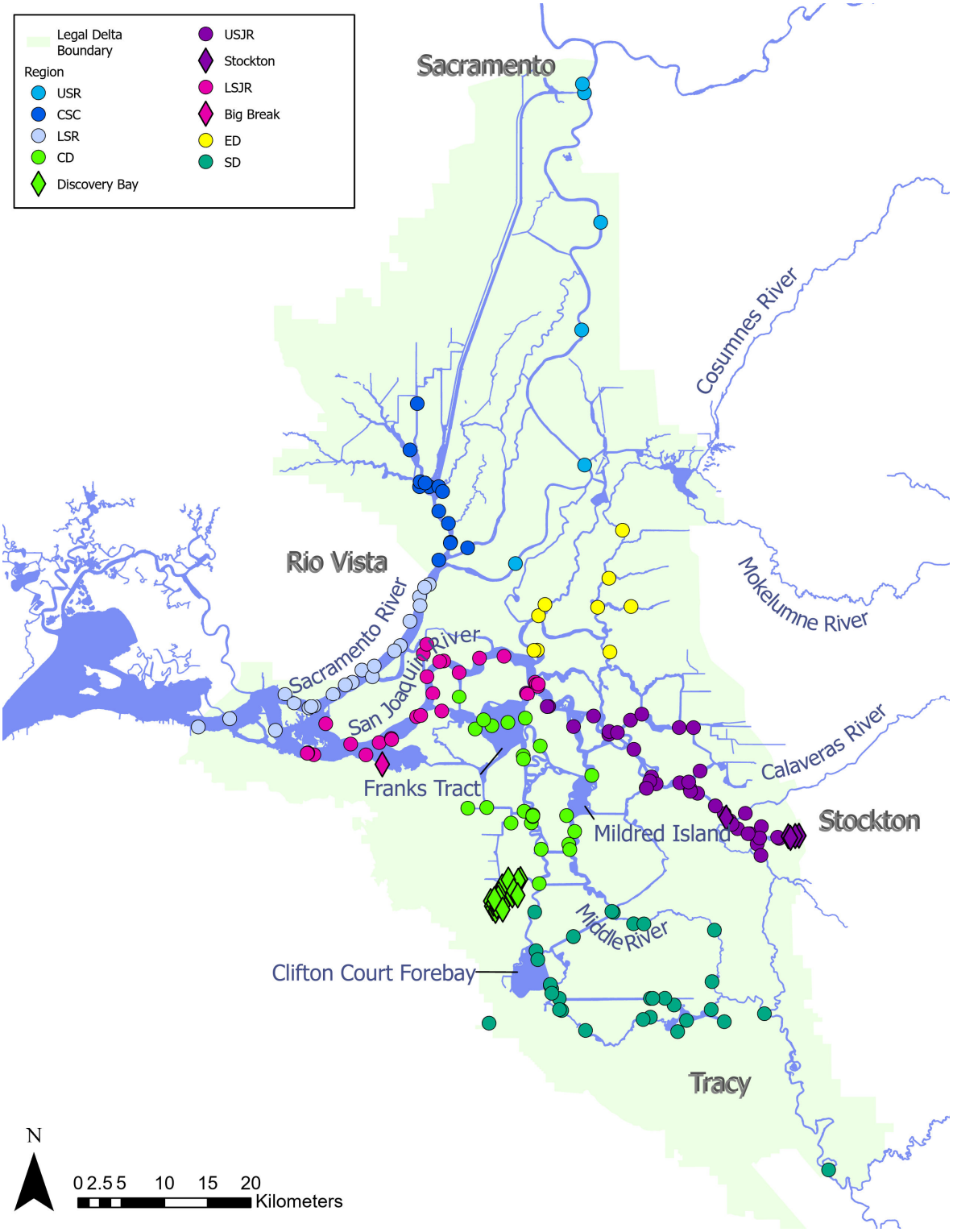

Figure 2 Map of the Sacramento San Joaquin Delta showing the regions used for the study analysis. Not all data types analyzed in this paper were available for every station; each station shown represents a location where at least one data type was collected. Regions are shown by *colored circles*; dead-end areas are shown by *colored diamonds* with color corresponding to the region where the dead-end sites are located. See Figure A3 for a map that categorizes all sites by habitat type. CSC = Cache Slough Complex, USR = upper Sacramento River, LSR = lower Sacramento River, CD = Central Delta, LSJR = lower San Joaquin River, USJR = upper San Joaquin River, SD = South Delta, ED = East Delta.

Table 1 Temporal and spatial information about existing programs that monitor parameters relevant to CHABs. The spatial scope describes the general areas the monitoring program oversees. Individual monitoring sites may have been added, removed, or moved by programs over time. Monitoring frequency may also have changed over time. The monitoring time-span column notes when the first relevant constituents to CHAB monitoring may have been added to these monitoring programs midway through the time-spans.

Agency	Program	Spatial Scope	Monitoring Frequency	Parameters	Monitoring Time-Span
CDWR	Environmental Monitoring Program (EMP)	San Pablo Bay, Suisun Bay, Suisun Marsh, Montezuma Slough, Sacramento River, San Joaquin River, Old and Middle rivers	At least monthly	Phytoplankton ID, MVI, Chl-*a*	1975–present
CDWR	Yolo Bypass Fish Monitoring Program	Yolo Bypass, Cache Slough Complex, Sacramento River	Variable, roughly monthly, typically December/ January through June	Phytoplankton ID, Chl-*a*	1998–present
CDWR	North Central Regional Office (NCRO)	South Delta, Central Delta, North Delta	Monthly	Phytoplankton ID, Chl-*a*	2019–present (FlowCam)
CDFW	Fish Restoration Program Effectiveness Monitoring Team	Cache Slough Complex, lower Sacramento River, Confluence, Suisun Bay, Suisun Marsh	Spring, summer, and fall	Phytoplankton ID, MVI, Chl-*a*	2015–present
USGS	California Water Science Center Biogeochemistry Group	Delta-wide during mapping surveys (30 sites), currently ~12 fixed stations but amount of sampling depends on funded projects	Monthly, spring, summer, fall	Phytoplankton ID, MVI, Chl-*a*, Algal Toxins	2018–present
USGS	SFB Research and Monitoring Program	San Francisco Bay, San Pablo Bay, Suisun Bay, and lower Sacramento River	Every 2 weeks, monthly, year-round	Phytoplankton ID, Chl-*a*	1992–present
State Water Board/ SFEI	HAB Satellite Analysis Tool	Statewide lakes and major water bodies including Cache Slough, Franks Tract and lower Sacramento and San Joaquin rivers	Composite 1- or 10-day pixel max	Cyanobacterial index, Chl-*a* (beta)	2016–present, (Cyanobacterial index); 2023-present (Chl-a)

Environmental Data Initiative (EDI) Delta Water Quality Integrated Dataset Package (*https://portal.edirepository.org/nis/mapbrowse?scope=edi&identifier=458*).

Microcystin toxin concentrations, and MVI scores

Data from each dataset were summarized from 2014 to 2022 for chl-*a*, *Microcystis* units, microcystins, and the MVI data, (defined in the MVI Background section below). qPCR were compiled from special studies conducted from 2014 to 2019 (Kurobe et al. 2022) as well as a special study conducted in 2021 (Preece, Otten, Cooke 2024; Preece et al. 2025). Microcystin data were collected from the East Bay Regional Park's routine cyanotoxin testing program, a special study by the Biogeochemistry Group at the USGS California Water Science Center, Central Valley Water Board HAB Freshwater and Estuarine Harmful Algal Bloom Program incident response data, Restore the Delta, a special study by Kurobe et al. (2022), special studies by CDWR, Central Valley Water Board and Bend Genetics, and a special study conducted on behalf of the City and Port of Stockton. *Microcystis* seedstock data was compiled and synthesized from a special study conducted by Preece et al. (2025). Although remote sensing data was not compiled for this effort it is also considered in this paper.

When possible, data was analyzed for the entire calendar year. However, qPCR data was

https://doi.org/10.15447/sfews.2026v24iss3art?

only available from May through December. Microcystin data was also not available for all months of all years. Additionally, data coverage varied by region, with some stations or areas having incomplete records across the study period.

Regional Analysis

To evaluate spatial and temporal patterns across study regions, we analyzed chl-*a*, microscopic *Microcystis* counts, qPCR results, MVI scores, and microcystin data. There were not sufficient *Microcystis* seedstock data to include in the regional analysis. All statistical analysis was completed in R version 4.5.0 (R Core Team 2025).

A Generalized Additive Mixed Model (GAMM) was used to model annual temporal variation in chl-*a* across six Delta regions, following the procedures of Zuur et al. (2009). Chl-*a* was natural log-transformed to meet the assumption of normality. A GAMM was selected to capture the non-linear dynamics of chl-*a* while accounting for spatial and temporal autocorrelation. Generalized additive models fit subsets of predictor variables using first-, second-, or third-order polynomials that are combined to represent complex non-linear patterns (Zuur et al. 2009). Chl-*a* was modeled as:

$$y_{jk[i]} = \beta_0 + s(\text{day of year}) + a_j + a_k + \varepsilon_{jk[i]}$$

$$a_j \sim N(0,\sigma^2 a_j) \text{ for } j=1...J_{station}$$

$$a_k \sim N(0,\sigma^2 a_k) \text{ for } k=1...K_{year}$$

$$\varepsilon \sim N(0, \sigma^2_\varepsilon)$$

where $y_{jk[i]}$ was the expected chlorophyll response value at station j in year k, β_0 was the intercept, s (day of year) was a cubic spline smoothing function capturing the nonlinear effect of day of year on chl-*a*, a_j was the random effect for station, a_k was the random effect for year, and $\varepsilon_{jk[i]}$ was the residual error for each year and station. An autoregressive correlation structure was used to account for autocorrelation between day of year and stations. The random effects a_j and a_k were assumed to be normal with a mean of 0 and variance of $\sigma^2 a_k$ and $\sigma^2 a_j$ for each station and year, respectively. $\varepsilon_{k[i]}$ was assumed to be normal with a mean of 0 and variance of σ^2_ε. We conducted our statistical modeling with the *mgcv* package version 1.9-3 (Wood 2004). The R^2 value for the chl-*a* model was 0.26 each, and the regional smoothing term *p*-values can be found in Appendix A. The interannual variability of the chl-*a* data lowers the R^2 value.

To estimate the maximum attainable phytoplankton biomass in each region, potential chl-*a* was calculated using the yield of chl-*a* based on concentration of N, which has shown remarkable consistency among varied systems, including the Delta (Gowen et al. 1992; Tett et al. 2003; Mussen et al. 2023).

Microcystis abundance measured by qPCR was compared across regions using a Kruskal–Wallis test, followed by a post-hoc Dunn's test with the Holm correction. To visualize *Microcystis* abundance by region, month, and year, qPCR-derived *Microcystis* 16S rRNA gene copy concentrations were plotted. For each Region–Month–Year combination, the maximum observed *Microcystis* concentration was assigned to one of five percentile categories (non-detect, ≤25th, 25th–50th, 50th–75th, >75th), with percentile thresholds calculated from all detectable values across the dataset.

A one-way analysis of variance (ANOVA) was conducted on the microcystin dataset to allow comparison of toxins across regions. To account for differences in water-year type (wet, above normal, below normal, dry, critical), a random effect term was included in the ANOVA model. The Sacramento Valley Hydrologic Classification Index was used to classify the water-year type (CDEC 2024). A Tukey post-hoc test was performed to compare differences between all regions. The distribution of microcystin occurrences within each region from June through November were described using a ridgeline plot. Actual means of

microcystin concentrations within each region were plotted on each ridgeline.

The *Microcystis* cell concentration data from the CDWR's Environmental Monitoring Program (EMP) were analyzed to assess spatial and temporal variability across regions of the Delta. These data were log-transformed to normalize the data, and monthly means were calculated after grouping by region, California water year (October 1 to September 30), and station. A one-way ANOVA was used to evaluate monthly differences, followed by a linear mixed-effects model (LMM) with the log-transformed means as the response variable, region as a fixed effect, and nested random effects for water year, month, and station (see Appendix A). For visualization, seasons were defined as follows: winter (December–February), spring (March–May), summer (June–August), and fall (September–November).

Microcystis measured by qPCR was compared across regions using a Kruskal–Wallis test followed by a post-hoc Dunn's test with the Holm correction.

Multivariate analysis was conducted to evaluate differences among months and regions, by considering combined variations of multiple water-quality parameters simultaneously to provide a more comprehensive understanding of CHAB patterns across regions. To assess differences in water-quality parameters among months during the primary bloom season (June–October) and across regions, we conducted a permutational multivariate analysis of variance (PERMANOVA) using the Bray–Curtis dissimilarity metric. Before analysis, data were averaged by month for each region, and all variables were standardized to ensure that parameters measured on different scales contributed equally to the analysis. Observations with missing values were removed to allow distance calculations. Pairwise PERMANOVAs were subsequently performed to identify specific months that differed significantly in overall water-quality composition. Analyses were implemented using the "adonis2" function in the *vegan* package (Oksanen et al. 2025) with 999 permutations.

Results of the multivariate analysis were used to inform the development of a heatmap for visual comparison of regions and parameters. Median values were calculated for each parameter–region combination, then scaled relative to the maximum median for each parameter.

Habitat Analysis

Habitat types were classified as described earlier: (1) dead-end channels and marinas; (2) flooded islands, shallow side channels, and sloughs; and (3) main channels (Figure 1). Data were limited for the habitat analysis because they were from special studies, because routine monitoring does not include the stations or parameters needed to conduct a habitat analysis. Dead-end habitats included in the analysis included Big Break, Discovery Bay, and Stockton Waterfront (Figure 2). The microcystin dataset comprised special studies and incident response sampling, except for Big Break and Clifton Court Forebay, which have routine monitoring. Incident response sampling, which tends to be triggered by visual bloom observations, may bias microcystin concentrations and detection frequencies upward at sites where it comprises most samples, such as Discovery Bay. In contrast, some special-study samples were collected regardless of bloom presence, which may result in a higher proportion of non-detects at those locations. There were sufficient data from special studies available to analyze microcystins and *Microcystis* seedstock by habitat type. Although there were insufficient data for a habitat analysis of MVI and qPCR, data from the Stockton Waterfront dead-end channel were included in the analysis.

Differences among habitat types were evaluated using a Kruskal–Wallis test, followed by Dunn's post hoc pairwise comparisons with Bonferroni-adjusted p-values. To assess variation in detection frequency among habitats, non-detects were analyzed using a Pearson's Chi-square test. The distribution of microcystin occurrences within each habitat type from June through November were described using a ridgeline plot. Actual

https://doi.org/10.15447/sfews.2026v24iss3art?

means of microcystin concentrations within each habitat type were plotted on each ridgeline.

RESULTS AND DISCUSSION OF PARAMETERS USED TO QUANTIFY CHABS

Chlorophyll-*a* and Accessory Pigment Concentrations

Background

Chl-*a* is considered a standard water-quality measurement, and is routinely collected in estuaries world-wide, including the San Francisco Estuary and the Delta (e.g., Jassby et al. 2002; Cloern and Jassby 2012; Cloern et al. 2014; Sutula et al. 2017). Chl-*a* is common to all phytoplankton, including eukaryotic phytoplankton, such as diatoms, and prokaryotic phytoplankton, such as cyanobacteria. In addition to chl-*a*, phytoplankton contain accessory pigments that are useful as taxonomic markers because they are unique within broader taxonomic phytoplankton groups (Mackey et al. 1996; Jeffrey et al. 2011; Kramer et al. 2022). These accessory pigments occur in specific ratios with chl-*a* in the cell (e.g., Mackey et al. 1996) and can be measured chemically (Hooker and Van Heukelem 2011) or via fluorescence (Bertone et al. 2018). For example, phycocyanin and phycoerythrin are pigment protein molecules unique to cyanobacteria, and detection of their fluorescence signal can be used to quantify cyanobacteria and CHAB biomass *in situ* as a fraction of total chl-*a*, with certain caveats (Bertone et al. 2018; Ma et al. 2022; Rousso et al. 2022).

Delta-Specific Analysis

Compared with other estuaries that have similar levels of nutrient loading, primary productivity and mean summertime chl-*a* concentrations in the Delta are considered low (Cloern et al. 2014). As a result, the Delta is classified as oligotrophic: i.e., annual primary production less than 100 g Carbon (C) m^2 yr^1 (Nixon 1995; Jassby et al. 2002; Cloern et al. 2014). Despite being an oligotrophic system, the Delta can experience high swings in chl-*a* concentration, reaching in some instances 20 times the mean concentration (Perry et al. 2023). Peak chl-*a* concentrations occurred primarily in spring and summer, with the highest values observed in 2015 and 2016. Data from 2017 and 2021 also showed elevated concentrations in some regions (Figure 3).

For example, there was a large increase in chl-*a* concentrations in spring of 2016 in the LSR, CD, and LSJR regions of the Delta. This event was driven by a large bloom of the chain-forming diatom *Aulacoseira granulata*, with chl-*a* concentrations reaching 75 µg chl-*a* L^{-1} (Jungbluth et al. 2021). The event began in March in the CSC region, but it was likely missed in our time-series because of the timing of sampling by the routine monitoring program (Jungbluth et al. 2021). Despite the absence of the 2016 spring bloom in the USJR and SD regions, these areas exhibited the highest summertime mean chl-*a* concentrations in our time-series during 2016. Mean summertime chl-*a* concentrations typically range from 4.0–12.0 µg L^{-1} in the SD region, but reached 40 µg L^{-1} in 2016 (Perry et al. 2023; Figure 3). The factors driving elevated summertime chl-*a* in 2016 remain unclear, but it was a below-normal water year that was preceded by a 4-year drought. Yet, water-year type alone does not explain why SD chl-*a* concentrations were so high in the summer of 2016, because chl-*a* concentrations in this area were very low during the 2020 to 2022 drought (Figure 3).

Because infrequent peaks in chl-*a* can skew mean values, median concentration better represents typical conditions in regions with episodic blooms. Lowest median summertime chl-*a* concentrations occur in the CSC region, followed by the LSR region, and the CD region (Table 2). This pattern is also reflected in the GAMM plot (Figure 4). In these regions, median July chl-*a* concentrations vary from 1.7 in the CSC to 3.2 µg L^{-1} in the CD (Table 2). The highest summertime chl-*a* occurs in the USJR and SD regions, where median July concentrations range from 4.3 in the USJR to 6.4 µg L^{-1} in the SD (Table 2). Both median and mean summertime chl-*a* concentrations are greatest in the SD region, where the channels experience less tidal exchange and longer residence times. The GAMM plot corroborates this pattern, with the highest

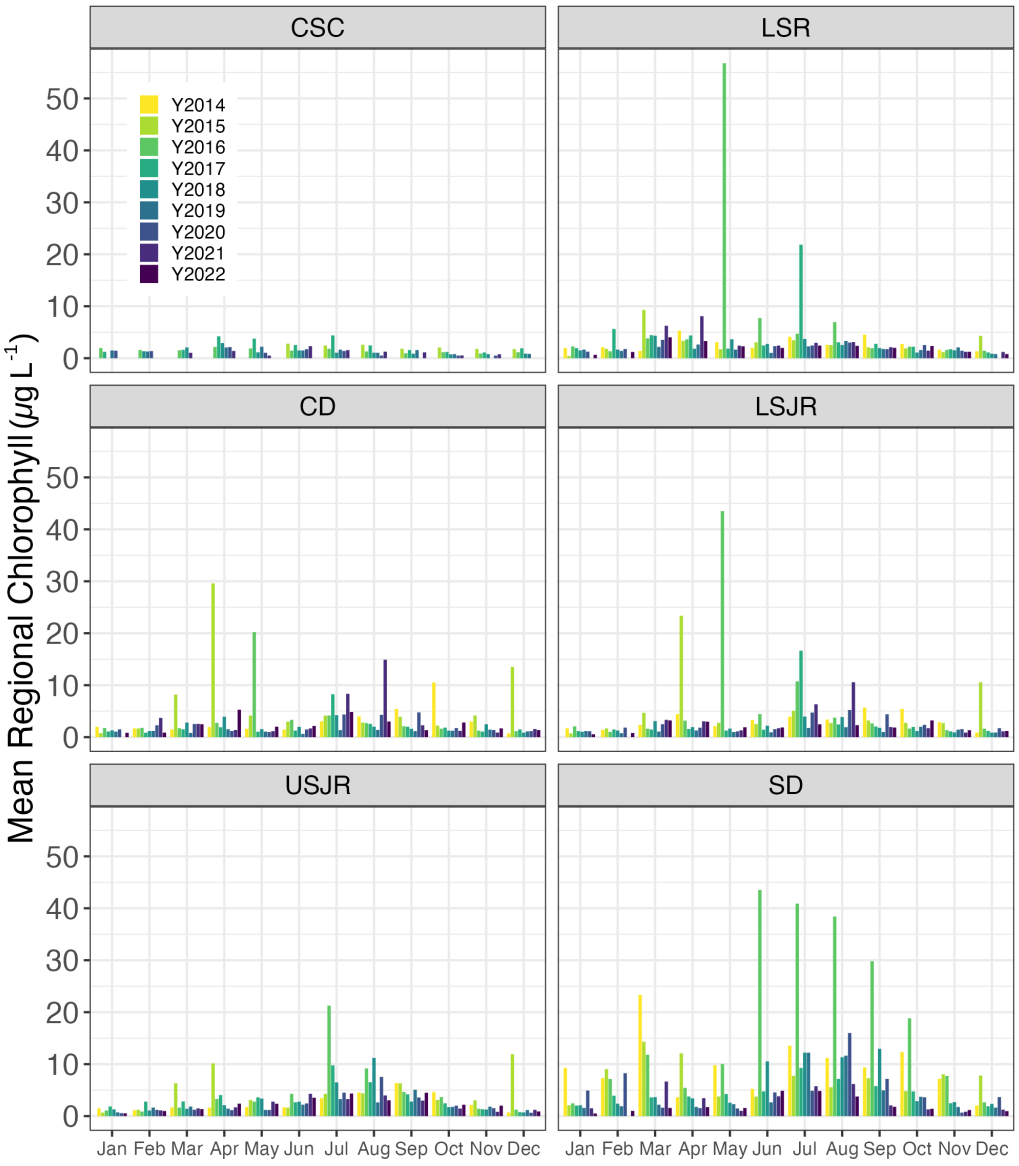

Figure 3 Mean monthly chl-*a* concentrations (μg L^{-1}) in six Delta regions by year from 2014–2022. CSC = Cache Slough Complex, LSR = lower Sacramento River, CD = Central Delta, LSJR = lower San Joaquin River, USJR = upper San Joaquin River, SD = South Delta. No data available for the East Delta (ED) or upper Sacramento River (USR) regions.

predicted chl-*a* in the SD and USJR compared to other Delta regions (Figure 4).

As a result of generally low chl-*a* concentrations paired with relatively high nutrient concentrations, potential chl-*a* was calculated to determine the magnitude of phytoplankton biomass that could accumulate if the residual nutrient pool was drawn down completely, as occurred in spring of 2016. This calculation demonstrates that the Delta phytoplankton community has "room to grow," particularly in the USJR and the SD regions (Figure 5). These two regions are also the regions with the highest measured chl-*a* concentrations.

Currently, the relationship between CHAB biomass and total phytoplankton biomass is not well understood for the Delta, and, moving into a warming future, it is not clear how much denser CHAB events could become. Combining chl-*a* measurements (indicator of total phytoplankton biomass) with a cyanobacteria-specific measurement (i.e., phycoerythin fluorescence or microscopy), can indicate the proportion of total phytoplankton biomass that comprise CHAB biomass and how this proportion may change over time. To date, chl-*a* concentration has not been a good indicator of CHAB occurrences in the Delta because *Microcystis* colonies are not evenly distributed throughout the water column, and

https://doi.org/10.15447/sfews.2026v24iss3art?

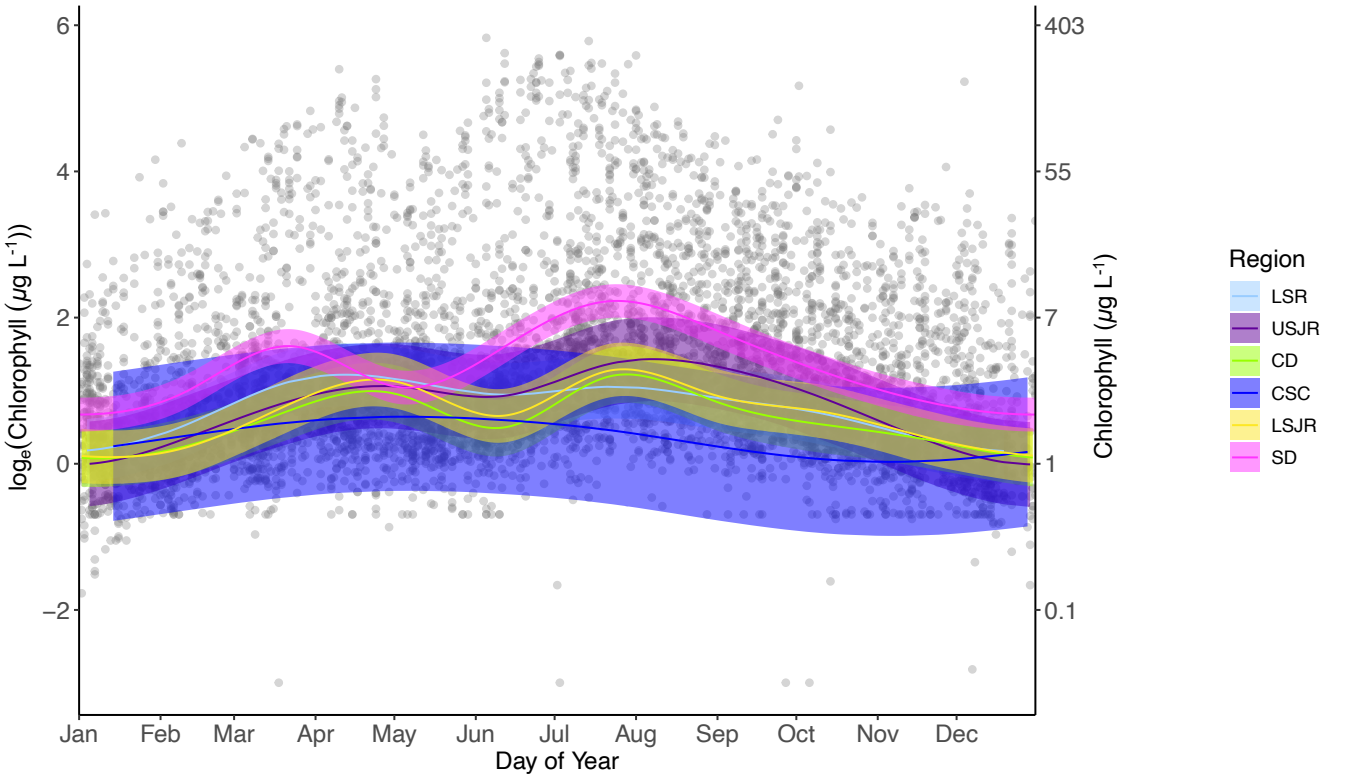

Figure 4 Observed log$_e$[Chlorophyll (μg L^{-1})] across the calendar year (*transparent gray points*) shown with Generalized Additive Mixed Models (GAMMs) predicted Delta chlorophyll-*a* per region (*colored lines*). Shown with 95% confidence intervals (transparent *colored polygons*). Right *y*-axis denote back-transformed chlorophyll-*a* (μg L^{-1}). CSC = Cache Slough Complex, LSR = lower Sacramento River, CD = Central Delta, LSJR = ower San Joaquin River, USJR = upper San Joaquin River, SD = South Delta. No data available for the East Delta (ED) region.

Table 2 Monthly median (mean±SE) chl-*a* (μg L^{-1}) concentrations by region in the Delta for years 2008–2022.

Month	CSC	LSR	CD	LSJR	USJR	SD
Jan	1.5 (1.5±0.2)	1.5 (1.5±0.1)	1.1 (1.3±0.1)	1.1 (1.3±0.1)	1.0 (1.1±0.1)	1.8 (3.4±0.5)
Feb	1.4 (1.4±0.1)	1.5 (2.0±0.3)	1.4 (1.6±0.2)	1.3 (1.3±0.1)	1.1 (1.3±0.2)	2.2 (6.0±0.9)
Mar	1.6 (1.6±0.2)	4.3 (4.6±0.4)	2.0 (2.9±0.6)	2.1 (2.6±0.3)	1.6 (2.4±0.7)	2.8 (9.0±1.4)
Apr	2.4 (2.4±0.4)	3.1 (4.3±0.5)	2.1 (6.7±1.8)	2.2 (6.1±1.5)	2.4 (3.2±0.6)	1.9 (5.0±0.7)
May	1.9 (1.8±0.4)	2.3 (7.6±2.9)	1.5 (4.5±1.3)	1.7 (6.9±2.1)	2.2 (2.6±0.3)	2.0 (4.8±1.0)
Jun	1.9 (2.1±0.2)	2.2 (2.7±0.3)	1.8 (2.0±0.2)	1.9 (2.3±0.2)	2.6 (2.7±0.2)	3.0 (10.1±2.3)
Jul	1.7 (2.3±0.4)	2.9 (4.7±1.0)	3.2 (4.5±0.5)	3.7 (5.9±0.8)	4.3 (6.7±1.5)	6.4 (13.2±1.9)
Aug	1.2 (1.4±0.3)	2.8 (3.2±0.3)	2.6 (4.1±0.5)	3.1 (4.1±0.5)	4.1 (6.0±0.9)	5.8 (13.4±1.5)
Sep	1.3 (1.3±0.2)	2.1 (2.3±0.2)	2.3 (2.9±0.3)	2.3 (3.0±0.2)	4.1 (4.6±0.5)	5.4 (10.9±1.1)
Oct	0.8 (1.0±0.2)	1.9 (2.0±0.1)	1.8 (3.2±1.1)	2.0 (2.6±0.2)	2.5 (2.6±0.3)	2.6 (6.8±1.4)
Nov	0.8 (1.0±0.3)	1.5 (1.5±0.1)	1.4 (2.0±0.3)	1.4 (1.7±0.1)	1.5 (1.7±0.2)	2.0 (4.5±0.6)
Dec	1.6 (1.4±0.2)	1.0 (1.4±0.2)	1.1 (2.9±0.6)	1.2 (2.5±0.5)	1.0 (2.4±1.0)	1.7 (3.4±0.4)

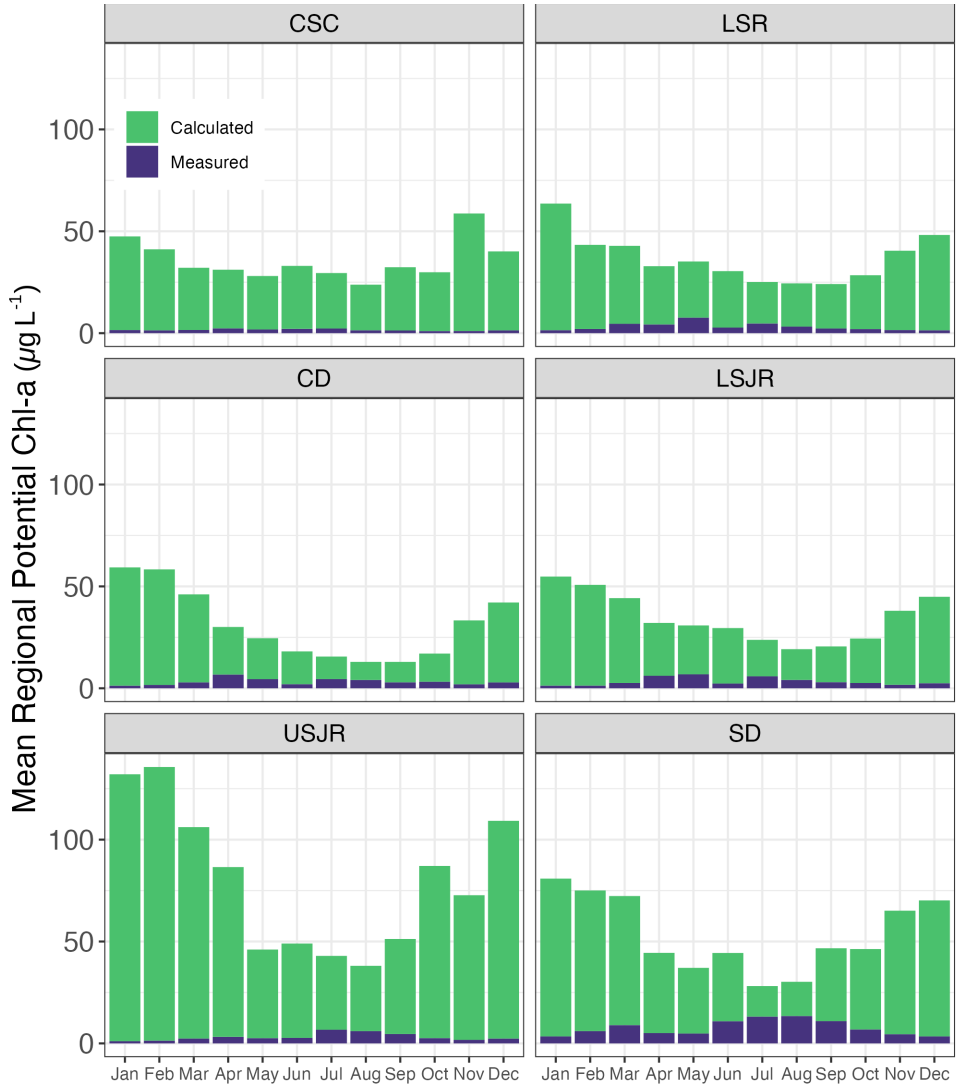

Figure 5 Mean measured and additional potential chl-*a* (μg L^{-1}) if the residual nutrient pool was drawn down in Delta regions by month from for the 2014–2022 time-period. CSC = Cache Slough Complex, LSR = Lower Sacramento River, SJR = San Joaquin River, CD = Central Delta, SD = South Delta. No data available for the East Delta (ED) or upper Sacramento River (USR) regions.

their buoyancy makes them difficult to capture consistently in grab samples. Additionally, samples collected at 1 m depth are not representative of total *Microcystis* biomass, which is typically distributed across the photic zone (Ted Flynn, pers. comm.).

4.2 Microscopy-Based Estimates of Cell Abundance

Background

Microscopy is commonly used for enumerating phytoplankton samples and can be used to determine cyanobacterial community composition and biomass by measuring the volumes of individual cells or colonies. Although microscopy is useful, it is a time-consuming process with variable results, depending on the complexity of the target species, the training of the taxonomist, and the existence of inter- and intra-expert agreements in species identification. As such, microscopy results may be especially challenging for evaluating statuses and trends if datasets generated by different microscopists are used.

https://doi.org/10.15447/sfews.2026v24iss3art?

Delta-Specific Analysis

To date, 16 different cyanobacteria genera have been identified in the Delta via microscopy (Spier et al. 2013; Lehman 2022; Richardson et al. 2023), with *Microcystis* typically dominating cyanobacteria biomass (Lehman et al. 2017, 2022). Microscopic enumeration of *Microcystis* colony units has been incorporated into routine monitoring at selected stations throughout the Delta. However, microscopy data are largely absent from areas with the most severe CHABs, such as Discovery Bay and the Stockton Waterfront.

Data from the EMP show that the abundances of *Microcystis* colonies tend to be the greatest in the SD and USJR regions, with lower concentrations in the CD and LSJR regions (Figure 6). Colony abundances decrease from the middle of the San Joaquin River toward the confluence. Consistent with this, the LSJR region has abundances an order of magnitude—or more—lower than the USJR. In the CSC and LSR regions, *Microcystis* colonies are typically not detected (Figure 6; Kimmerer et al. 2018).

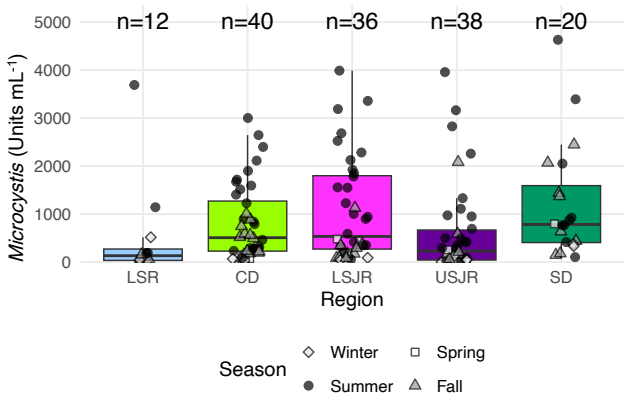

Figure 6 Abundance of *Microcystis* colony units (units mL^{-1}) in five Delta regions by month in the years 2014–2022. Colony units are used because individual cells cannot be reliably enumerated within intact mucilaginous colonies. *Jittered points* show individual measurements, and *color and shape of the point* corresponds to the season in which the sample was collected. Winter = December–February, Spring = March–May, Summer = June–August, Fall = September–November. LSR = lower Sacramento River, CD = Central Delta, LSJR = lower San Joaquin River, USJR = upper San Joaquin River, SD = South Delta. No data were available for the East Delta (ED), upper Sacramento River (USR), or Cache Slough

Gene Abundance as a Proxy for Cell Density

Background

As an alternative to microscopy, molecular methods are increasingly used to monitor cyanobacteria in water bodies worldwide (e.g., Moreira et al. 2014, 2022). High throughput sequencing of housekeeping genes such as the bacterial 16S rRNA gene (e.g., Caporaso et al. 2010) or cyanobacteria-specific conserved genes such as the phycocyanin locus (cpcBA) (Neilan et al. 1995) can be used to profile microbial communities (including cyanobacteria) and estimate the relative abundance of each taxon. For quantitative assessments of key organisms or specific functional genes (e.g., toxigenicity), real-time qPCR enables absolute quantification of genes. When single-copy genes—such as phycocyanin or cyanotoxin genes—are targeted, then the qPCR results represent cell equivalents. A strength of molecular methods over microscopy is the reproducibility of data, since user subjectivity is not a factor. Additionally, cells that have separated from colonies or are otherwise difficult to distinguish microscopically may be missed in microscope counts. For example, single *Microcystis* cells detached from colonies are often missed in microscope counts but are still captured during filtration and can be analyzed molecularly.

Delta-Specific Analysis

From 2014 to 2019, the CDWR's EMP program conducted routine monitoring that incorporated qPCR measurements of total cyanobacteria (16S rRNA gene) as well as the primary bloom-forming and the potentially toxigenic cyanobacteria genera *Microcystis*, *Aphanizomenon*, and *Dolichospermum* (Lehman et al. 2017) (Figure 7). The qPCR results indicated that *Microcystis*, *Aphanizomenon*, and *Dolichospermum* were minor components of the total cyanobacteria community. Yet, microscopic analysis of size-fractionated (>10 um) samples indicated that *Microcystis* often comprised 50% or more of the cyanobacteria in this size class. Combined, these data suggest that the majority of cyanobacteria across all size classes (i.e., unfractionated whole water) are actually small-cell, non-colonial

picocyanobacteria that are poorly detected by microscopy. Using high-throughput amplicon sequencing, Preece, Otten, Cooke 2024 observed that *Cyanobium*, a picocyanobacterium, was identified as the most abundant cyanobacteria genus across the Delta. Other studies have noted *Cyanobium*, as well as *Synechococcus* sp., to be present in Delta water samples (Kimmerer et al. 2018; Lehman 2022). These unicellular cyanobacteria are difficult to identify and generally not considered nuisance populations, and are thus commonly discounted in surveys of cyanobacterial communities, despite their contributing to total chlorophyll concentrations. Additionally, while most picocyanobacteria are considered to be ubiquitous and generally benign, there are reports of some strains producing cyanotoxins (c.f., Vareli et al 2012; Kopfmann et al. 2016).

Based on the qPCR dataset (Figure 7), *Microcystis* was highest in 2014, 2016, and 2021, all of which were drought years. Generally, *Microcystis* was lowest in 2017 and 2019, which were the two wettest years in the dataset, and in most areas there were cooler mean water temperatures (see Preece et al., this issue). *Microcystis* was highest in the dead-end channels and marinas in the Stockton Waterfront and Discovery Bay (Kruskal–Wallis; $p = 0.04$ to < 0.001) compared to all other regions. *Microcystis* was also significantly higher in the CD, USJR, and SD compared to the LSR (Kruskal–Wallis; $p < 0.001$).

Figure 7 qPCR estimates of monthly *Microcystis* concentration (^{16}S rRNA gene copies mL^{-1}) across regions and years. Tiles indicate the maximum percentile category of *Microcystis* per Region–Month–Year: non-detect (*grey*), ≤ 25th percentile, 25th–50th percentile, 50th–75th percentile, and > 75th percentile, with percentile thresholds computed from all detectable values. *Jittered circles* show individual sample measurements within each tile, highlighting within-month variation, with multiple samples per month slightly offset for visibility. The *color of the jittered circle* follows the same color scale as the legend. LSJR = lower San Joaquin River, USJR = upper San Joaquin River. No data available for Cache Slough Complex (CSC) or upper Sacramento River (USR) regions.

https://doi.org/10.15447/sfews.2026v24iss3art?

Microcystis Visual Index

Background

Microcystis sp. forms colonies in the water that vary in size from a few cells that cannot be seen without a microscope to large flakes composed of thousands of cells that are clearly visible with the naked eye. Studies have shown that mixing intensity can influence size and density of colonies, with intermittent and moderate mixing promoting formation of larger colonies (Xiao et al. 2018; Le et al. 2022).

Unique to the Delta is the development and implementation of an index known as the *Microcystis* Visual Index (MVI) to rank the relative density of visible *Microcystis* colonies in the water. The MVI gives a general idea of when and where blooms of *Microcystis* occur in the Delta. The density of colonies in the water or in a bucket are ranked according to a scale from 1 to 5 (i.e., R1 to R5) where R1 is absent and R5 is relatively high as depicted in Figure 8.

Delta-Specific Analysis

The MVI offers the most extensive record of CHAB conditions across the Delta, because these data can be collected during routine field activities without specialized equipment, and are thus inexpensive to obtain. The MVI also provides the broadest spatial and temporal coverage of CHAB observations across the Delta. These data have been collected monthly at discrete stations since approximately 2007 by the CDWR and CDFW. Other researchers and agencies also collect MVI data opportunistically. Since the majority of MVI data have been collected at established monitoring stations, observations for this parameter are primarily limited to main channel habitats, with some coverage of flooded island and side-channel areas. Limited MVI data from a special study in the dead-end habitat near the Stockton Waterfront were also included in the following analysis. The highest MVI rankings (i.e., R4 and R5) have occurred almost exclusively during July through September, and most frequently in the CD and USJR regions, followed by the SD region (Figure 9). These observations are consistent with the greatest mean summertime *Microcystis* colony abundances by region presented in Figure 4.

Examining absence (i.e., level R1) vs. presence (Levels R2 to R5) over the bloom season reveals two distinct regional patterns. In the CD, LSJR, USJR, and SD regions, *Microcystis* is absent until May, after which detections increase to a maximum in September before declining through November (Figure 9). In contrast, in the CSC, LSR, and ED regions, presences peak briefly in June or July before declining through the remainder of summer (Figure 9).

This regional divergence, a later seasonal peak in the CD, LSJR, USJR, and SD regions versus an earlier peak in the CSC, LSR, and ED regions, may reflect regional differences in what drives *Microcystis* colony density change. The two drivers

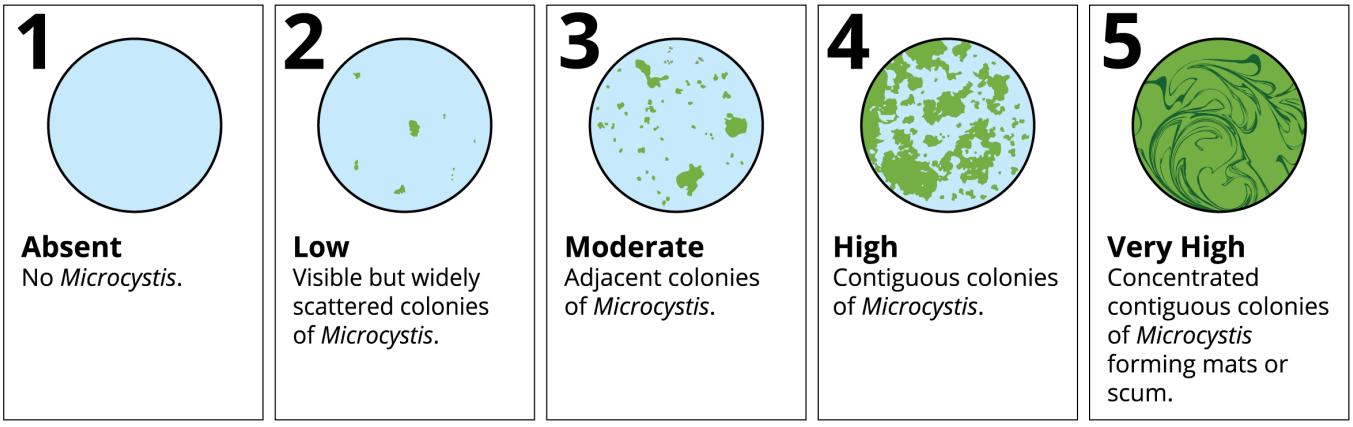

Figure 8 *Microcystis* Visual Index (MVI) ranking scale, R1–R5. *Source: Figure from Flynn et al. 2022.*

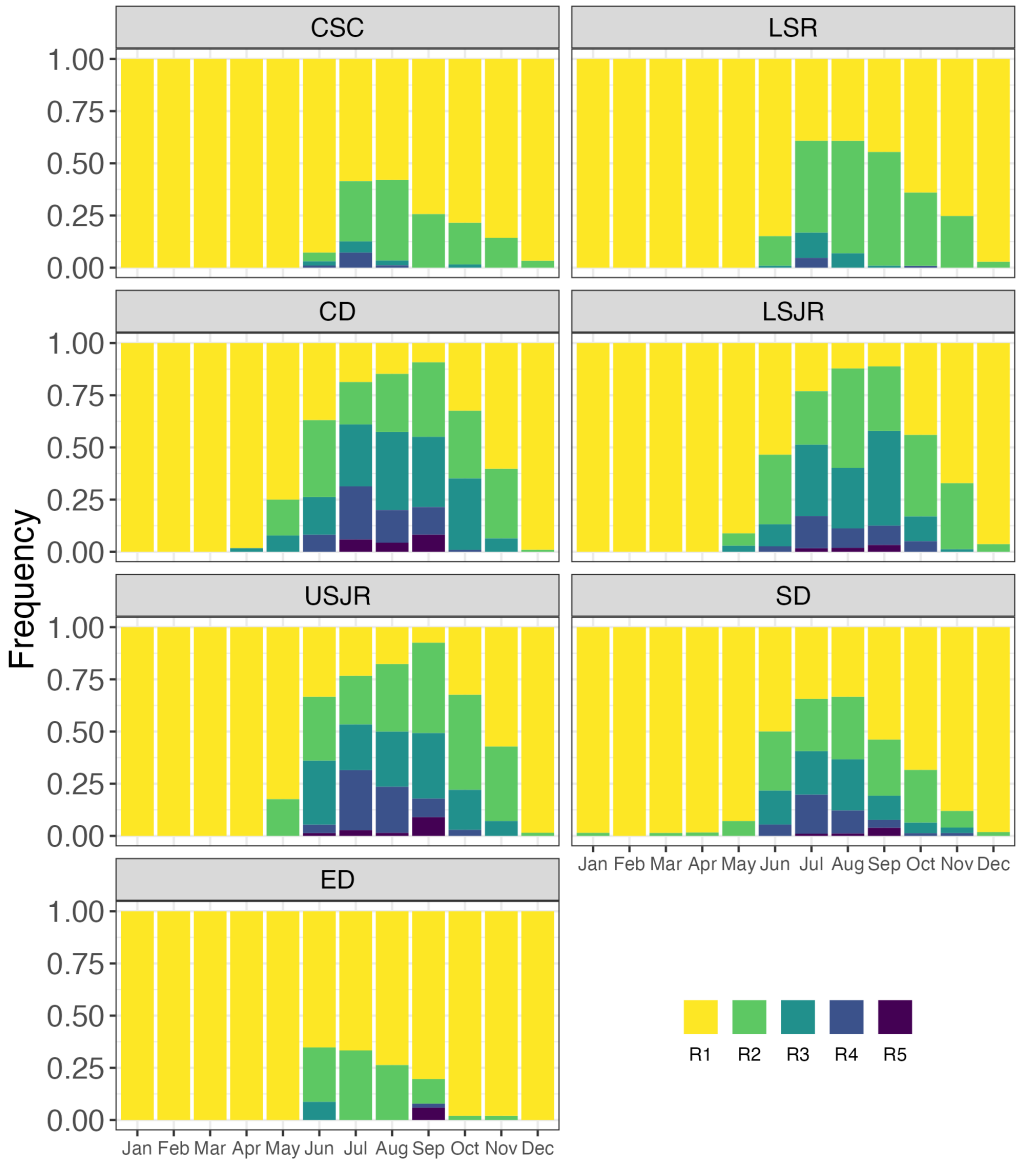

Figure 9 Fraction of *Microcystis* Visual Index (MVI) scales R1 through R5, where R1 is no colonies observed (i.e., absent) and R5 is contiguous colony density (i.e., scum formation) during all months for the years 2014–2022. CSC = Cache Slough Complex, LSR = Lower Sacramento River, CD = Central Delta, LSJR = lower San Joaquin River, USJR = upper San Joaquin River, SD = South Delta, ED = East Delta. There was not sufficient data available for upper Sacramento River (USR) region.

of an increase in colony density are (1) growth of *Microcystis* within a region, and (2) advection of colonies into a region from neighboring areas or, possibly, regions (Otten et al. 2015; Phlips et al. 2025). We hypothesize that autochthonous growth drives *Microcystis* abundance in dead-end areas, channel margins, and other shallow, slower-moving areas (i.e., the "growing areas"), whereas cell import drives abundance in deeper and faster moving areas of the Delta (i.e., the "advective areas"). Regions such as the CD, LSJR, USJR, and SD, which have a higher proportion of growing areas, may therefore support greater and more sustained local growth throughout the summer season. In contrast, it is still unclear what mechanisms are responsible for the reduced *Microcystis* presence observed in the CSC and ED regions in late summer. However, this decline may be linked to local habitat constraints or hydrodynamic conditions that limit sustained

https://doi.org/10.15447/sfews.2026v24iss3art?

bloom development in these regions. For example, these regions have fewer growing areas and may be more susceptible to flushing or light and nutrient conditions that become less favorable as summer progresses. Hydrodynamic modeling could help test what drives these regional differences in seasonal bloom patterns.

Our analysis demonstrates that CHABs do not occur in the main channels of the CSC, the LSR, and the ED where monitoring has been primarily concentrated (Figures 10A–10C). However, limited sampling in edge-water and side-channel habitats means these less-monitored areas may not be fully represented in the existing dataset. Main channels of the CSC, LSR, and ED either have high turbidity, a well-flushed deeper water column, or a combination thereof, that does not support CHABs. In contrast, the main channels in the CD such as Old River, and the USJR (San Joaquin River) do support *Microcystis* at intermediate concentrations (Figure 10). But these latter channels do not frequently produce the dense contiguous *Microcystis* biomass (i.e., level R5 on the MVI scale) that are reported in the dead-end channels and marinas such as the Stockton Waterfront (Figure 10). Main channels in the CD and USJR support frequent R3 and R4 occurrences (Figure 10).

Cyanotoxins

Background

Growth of CHAB species can negatively affect aquatic biota and the use of Delta waters through the production of cyanotoxins (Carmichael 1992; Chorus and Welker 2021), which are bioactive compounds with varying toxicities and modes of

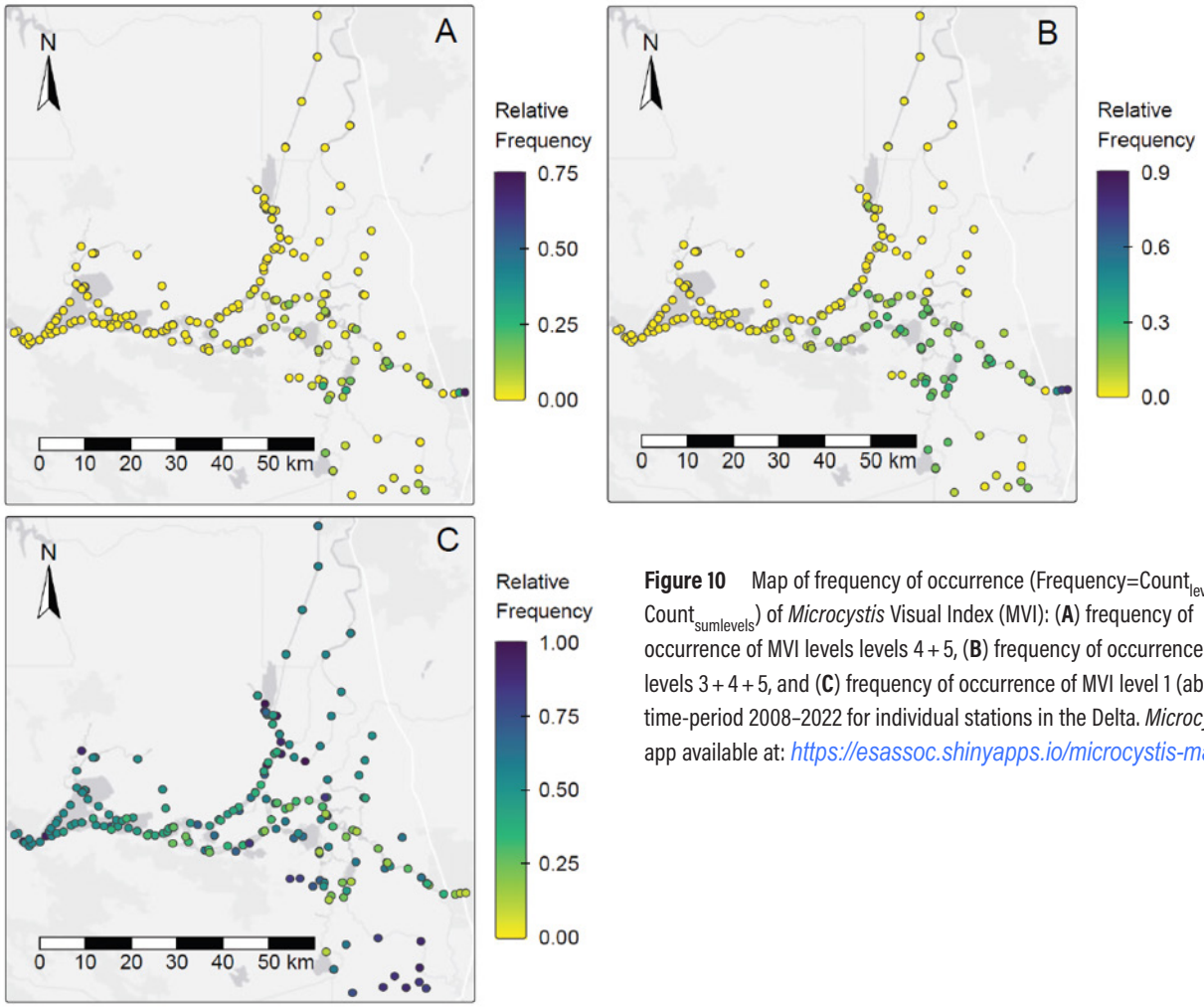

Figure 10 Map of frequency of occurrence (Frequency=$Count_{level}$/$Count_{sumlevels}$) of *Microcystis* Visual Index (MVI): (**A**) frequency of occurrence of MVI levels levels 4 + 5, (**B**) frequency of occurrence of MVI levels 3 + 4 + 5, and (**C**) frequency of occurrence of MVI level 1 (absent). For time-period 2008–2022 for individual stations in the Delta. *Microcystis* shiny app available at: *https://esassoc.shinyapps.io/microcystis-map/*).

action. These include liver toxins, neurotoxins, and dermatoxins. Concomitant with CHAB events, cyanotoxins have been detected in numerous water bodies worldwide. Hepatotoxic microcystins are recognized as the most common global cyanotoxin in freshwater systems (Harke et al. 2016; Preece et al. 2017; Preece, Otten, Cooke 2024). For a synthesis of marine and brackish HAB toxins in the San Francisco Estuary see Kudela et al. 2023.

In most cases, the majority of cyanotoxin will be stored intra-cellularly, therefore sampling efforts—especially for public health monitoring—typically target visual accumulations of potentially toxic cyanobacteria. In lacustrine environments, this typically means a water sample is collected from near shore, at the surface. Grab samples are the standard procedure identified by regulatory and health agencies to measure cyanotoxins in surface waters (US EPA 2023; CDC 2021; CWQMC 2026) but only represent a snapshot of water quality at a given time and place, and may miss cyanotoxins that are typically ephemeral and episodic (e.g., Howard et al. 2017).

Integrated and passive sampling approaches have increased in popularity because they can be used to effectively monitor cyanotoxins when grab samples may not be sufficient to capture a toxin event (Kudela 2017). The most common passive samplers used in cyanotoxin monitoring are solid phase adsorption toxin tracking samplers (SPATTs), which are exposed to water for longer durations and integrate toxins over time. Grab and SPATT sampling methods are not comparable to one another, but are complementary (e.g., Kudela 2011; Berg and Sutula 2015; Howard et al. 2017; Peacock et al. 2018). Other cyanotoxin monitoring techniques include filtering larger volumes of water, using shellfish as integrated toxin samplers (Preece, Otten, Cooke et al. 2024), or measuring cyanotoxin in sediments (Loaiza–González et al. 2024).

Delta-Specific Analysis

Because of the high costs associated with toxin analyses, cyanotoxin monitoring has generally been associated with special studies or by incident response sampling. Toxin analysis in the Delta has generally been conducted on surface water grab samples, although more recently SPATT samplers have become incorporated into some discrete monitoring stations and into boat-based mapping surveys (e.g., Bouma–Gregson et al. 2025). To date, microcystins have been the most monitored and detected cyanotoxin class throughout the Delta (Lehman et al. 2017, 2022; Preece, Otten, Cooke et al. 2024; Kudela et al. 2023), with concentrations attributed solely to *Microcystis* (Otten et al. 2017; Preece, Otten, Cooke et al. 2024). In addition to being detected in water samples and SPATT samplers, microcystins have also been found in sediments, zooplankton, fish, and shellfish within the Delta (Lehman et al. 2010; Bolotaolo et al. 2020). Tissue lesions consistent with liver toxins were documented in Inland Silversides (*Menidia beryllina*) and in juvenile Striped Bass (*Morone saxatilis*) caught during *Microcystis* blooms (Lehman et al. 2010). More recently, Preece, Otten, Cooke et al. (2024) reported widespread microcystin contamination of Asian clams and crayfish collected from various locations across the Delta between 2020 and 2023. The same study also analyzed samples for saxitoxins but found none in Asian clams or in water grab samples from ten sites across the Delta.

Low concentrations of anatoxin-a, saxitoxin, lyngbyatoxin, cylindrospermopsin, and anabaenopeptins have been detected occasionally where short-term studies funded analysis of additional toxins besides microcystins (Lehman et al. 2005, 2010, 2022; Mioni et al. 2011; Preece, Otten, Cooke 2024; Bouma–Gregson et al. 2025). The only routine cyanotoxin monitoring program that tests regularly for cylindrospermopsin and anatoxin-a is at Clifton Court Forebay and the Banks Pumping Plant, but between 2014 and 2022 all water grab samples were non-detectable for these toxins (Brianne Sakata, pers. comm.). While these grab samples may seem limited, they provide meaningful information because Clifton Court and Banks are integrator sites for water that flows to the pumps from many areas of the Delta.

https://doi.org/10.15447/sfews.2026v24iss3art?

Generally, toxins other than microcystins have been detected only via SPATT samplers, which suggests that SPATT samplers are more likely to capture toxins that occur at lower concentrations compared to water grab samples (Kudela 2017). Because toxin monitoring has primarily focused on measuring microcystin, and SPATT samplers have only been used over the past few years, it is unknown if other toxins are newer to the system or if the toxins have been missed because of a lack of monitoring or by relying only on water grab samples. However, SPATT effectiveness depends on resin type. HP20 resin, which is the most common resin used in SPATTs, is effective for microcystin and saxitoxin but less suitable for anatoxin-a and cylindrospermopsin. Strata-X works best for anatoxin-a, and no optimal resin has been identified for cylindrospermopsin. Thus, a single SPATT bag cannot reliably capture all toxin classes, especially uncommon toxins such as lyngbyatoxin and anabaenopeptin. Therefore, comprehensive cyanotoxin monitoring would ideally combine water grab samples with multiple SPATT resin types to ensure detection across all toxin classes.

Microcystin data from water grab samples were compiled from special studies, response monitoring, and routine monitoring programs conducted between 2014 and 2022. A total of 1,798 data points were organized by region for analysis (Figures 11 and 12). Of these, 43% (775 grab samples) had detectable microcystin concentrations. Only 24 detections (1%) occurred between December and May, with nearly half of the winter and spring detections concentrated at Big Break ($n = 9$), where the highest concentration was 2.3 µg L^{-1} in December 2020. There were 11 microcystin detections in May, but 3 of these are from a single date in 2022 along the Stockton Waterfront ($n = 3$), where samples ranged from 0.27 to 1 µg L^{-1}. All the other December to May samples were below the California caution trigger level of 0.8 µg L^{-1}. Notably, 1,190 samples (66%) were collected during the drought years of 2020 to 2022, indicating an increase in microcystin monitoring efforts in recent years (Figure 11).

A one-way ANOVA revealed a significant effect of region on log-transformed microcystin concentrations ($p < 0.001$). Post-hoc pairwise comparisons using Tukey's honestly signifcant difference (HSD) test showed that Big Break, Discovery Bay, and Stockton Waterfront consistently had significantly higher microcystin concentrations ($p < 0.001$) compared to all other regions. Stockton Waterfront had significantly higher microcystin concentrations than Big Break ($p < 0.001$), but not Discovery Bay ($p = 0.0721$). Big Break and Discovery Bay were also not significantly different from one another ($p = 0.2681$). At East Bay Regional Parks, which collects Big Break samples for microcystin testing, protocols specify that samples testing at 50 µg L^{-1} are not diluted further. As a result, 50 µg L^{-1} is the highest reported microcystin concentration at Big Break, although the true maximum is unknown. This may have led to the outcome in our analysis that showed the Stockton Waterfront had significantly higher microcystin concentrations than the Big Break site.

The USJR, CD, and SD also had significantly ($p < 0.001$) elevated microcystin concentrations compared to the ED, CSC, LSR, and USR (Figure 12). There was no significant difference in toxin concentrations between the USJR, CD, and SD. The highest microcystin concentration in these regions was a sample collected in July 2021 in the USJR region that contained 298 µg L^{-1} of microcystin. This sample was taken at Windmill Cove, which has been identified as a dead-end channel habitat. In fact, of the 44 samples that exceeded the California recreational exposure trigger levels Danger trigger of 20.0 µg L^{-1}, 42 of the samples were from the dead-end channel habitats of Big Break, Discovery Bay, and Stockton Waterfront. In contrast, in open-water areas of the Delta where dispersed flakes of *Microcystis* dominate, toxin concentrations are typically below California's Danger trigger (i.e., 20 µg L^{-1}) and generally below the California Warning trigger of 6 µg L^{-1} (Lehman et al. 2017; CDWR, unpublished data, unreferenced, see "Notes"; Preece, Otten, Cooke et al. 2024; Preece, Otten, Cooke et al. 2024; Figure 11). Concentrations are also frequently below the California Caution

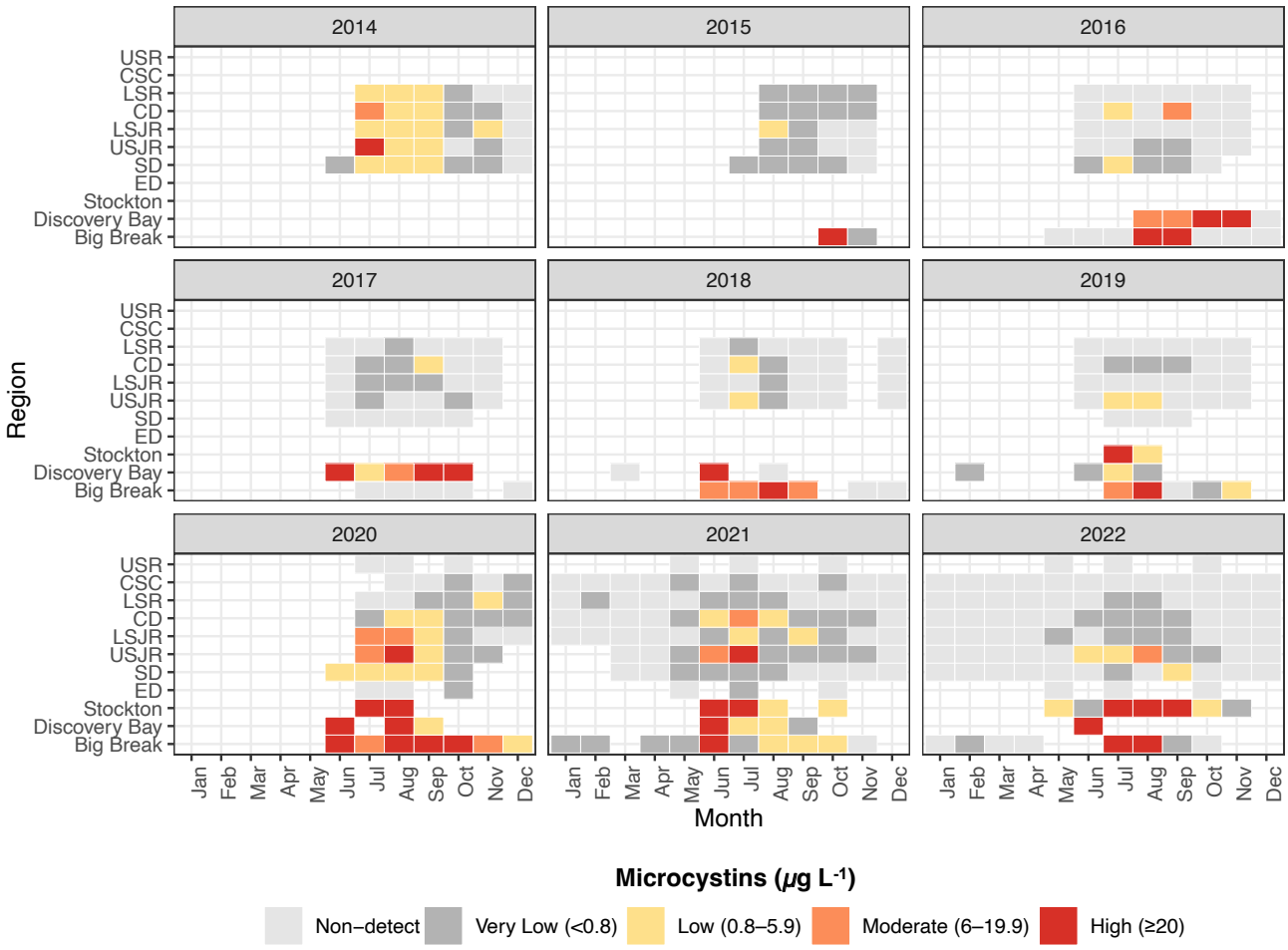

Figure 11 Monthly maximum microcystin concentrations (μg L^{-1}) in grab samples across regions from (2014–2022). *Colors* correspond to categories of non-detect sample, very low, low, moderate, and high concentrations. These categories are based on the California trigger levels for recreational exposure to microcystins. Only months with samples are shown; *white tiles* indicate no samples. *Facets* represent years, illustrating temporal and spatial variability in microcystin occurrence. *Tiles* represent 1 to 36 samples. USR = upper Sacramento River, CSC = Cache Slough Complex, LSR = lower Sacramento River, CD = Central Delta, LSJR = lower San Joaquin River, USJR = upper San Joaquin River, SD = South Delta, ED = East Delta, Stockton = Stockton Waterfront.

trigger of 0.8 μg L^{-1} (Lehman et al. 2017, 2022). However, this is a limited dataset and cannot be extrapolated to all open-water areas of the Delta.

The ridgeline plot in Figure 12 shows the distribution of microcystin concentrations by region. Only Big Break, Discovery Bay, and Stockton Waterfront exceed the California Danger trigger regularly. These locations also typically trigger monitoring only if a bloom is visually present; as such, there are fewer non-detects in these datasets. Nevertheless, these are also the areas of the Delta that more routinely have cyanobacteria scum present.

In addition to examining regional differences, we also assessed how microcystin concentrations varied across different habitat types (Figure 13; Table 3). Considering only detected values, microcystin concentrations differed significantly among habitats (Kruskal–Wallis; $p < 0.001$). Pairwise comparisons indicated significant differences among all habitat types, with dead-end habitats exhibiting significantly higher concentrations than the others (Dunn's test, adjusted P-values: dead-end vs. flooded island and side channels = 0.027; dead-end vs. main channel $< 1 \times 10^{-28}$; flooded island and side channels vs. main channel = 1.9×10^{-5}). Detection frequency

https://doi.org/10.15447/sfews.2026v24iss3art?

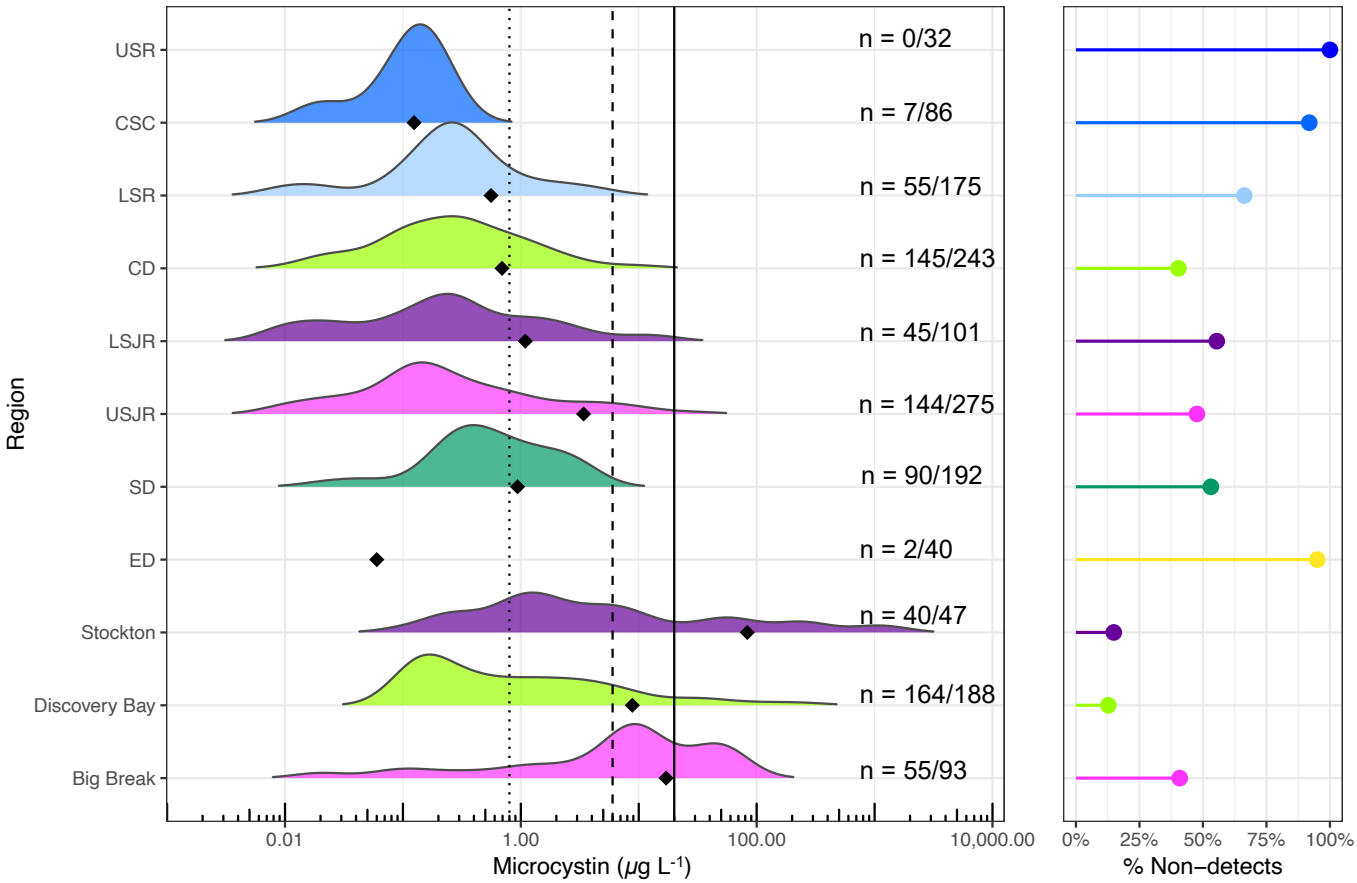

Figure 12 Total microcystin concentrations in water grab samples from June to November (2014–2022) are shown across regions. The ridge plot (*left*) depicts the distribution of detected concentrations (μg L^{-1}) on a log10 scale, with *black diamonds* marking mean values and *text annotations* indicating the number of positive detections relative to total samples (n = positive/total). The lollipop plot (*right*) shows the percentage of non-detect samples, highlighting differences in non-detect frequencies among regions. *Vertical lines* represent California recreational exposure trigger levels for microcystins (Caution at 0.8, Warning at 6, and Danger at 20 μg L^{-1}). There were only two positive detections in the East Delta and no positive detections in the upper Sacramento River so there was not sufficient data to develop a ridgeline for these regions. USR = upper Sacramento River, CSC = Cache Slough Complex, LSR = lower Sacramento River, CD = Central Delta, LSJR = lower San Joaquin River; USJR = upper San Joaquin River, SD = South Delta, ED = East Delta, Stockton = Stockton Waterfront.

also differed significantly among habitats, with dead-end sites showing the fewest non-detects and flooded island and side channel sites the most (Pearson's Chi-square test, $X^2 = 137.6$, df = 2, $p < 0.001$), which is summarized in the adjacent lollipop plot that shows the proportion of non-detects. Together, these results highlight that both the likelihood of detection and the magnitude of detected microcystin vary with habitat type (Table 3).

Cyanobacteria Seedstock

Background

Cyanobacteria cells in the water column are subject to a range of fates, including physical export, death, or dormancy. Dormant cells enter a vegetative state and sink out of the water column and into the sediment. Overwintering vegetative *Microcystis* colonies remain photosynthetically active and re-enter the water column through active re-suspension when environmental factors provide favorable growth conditions or through passive wind-induced re-suspension (Verspagen et al. 2005). Once established in a system, this

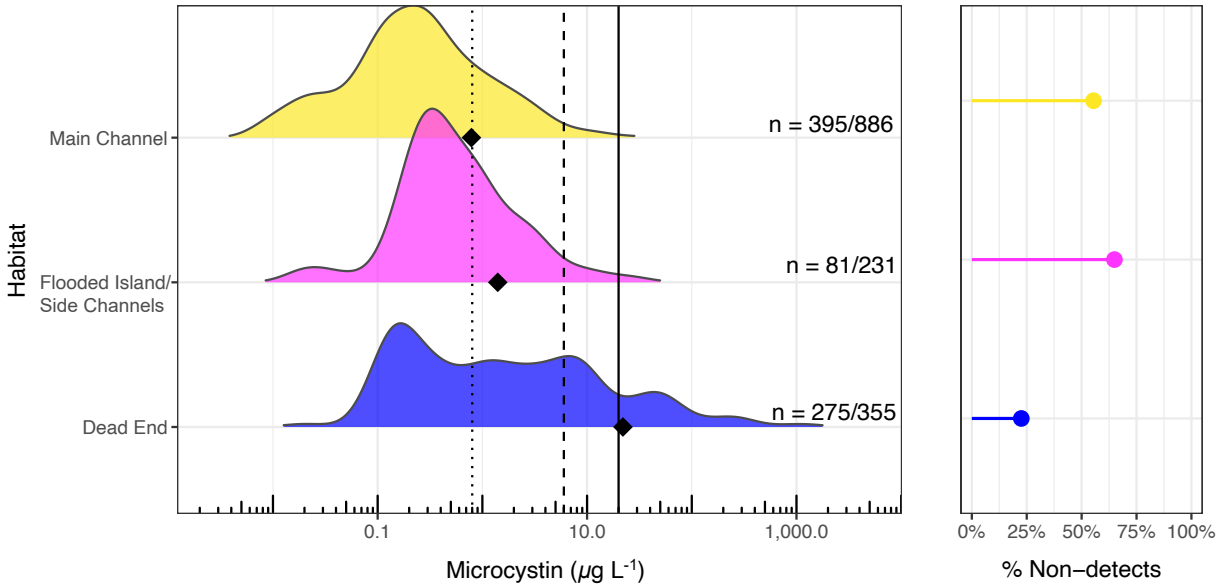

Figure 13 Total microcystin concentrations in water grab samples from June to November (2014–2022) are shown by habitat types. The ridge plot (*left*) depicts the distribution of detected concentrations (µg L^{-1}) on a log10 scale, with *black diamonds* marking mean values and text annotations indicating the number of positive detections relative to total samples (n = positive/total). The lollipop plot (*right*) shows the percentage of non-detect samples, highlighting differences in non-detect frequencies among regions. *Vertical lines* represent California recreational exposure trigger levels for microcystins (Caution at 0.8, Warning at 6, and Danger at 20 µg L^{-1}).

Table 3 Percentage of microcystin grab samples exceeding California recreational exposure trigger levels by habitat type, June–November 2014–2022

Habitat type	% > Caution (0.8 µg L^{-1})	% > Warning (6 µg L^{-1})	% > Danger (20 µg L^{-1})
Dead-end	40%	20%	10%
Flooded islands and side channels	10%	1%	0.4%
Main channels	7%	0.6%	0.1%

overwintering strategy allows cyanobacteria cells to form recurring, seasonal blooms (Cai et al. 2021). However, this overwintering strategy depends on the retention of viable cells within the system, because export via hydrodynamic transport or deep burial in the sediment may reduce the local seedstock available for bloom initiation the following season.

Delta-Specific Analysis

Studies that address overwintering Microcystis cells in the Delta are limited, and thus analyses performed in other sections of this paper are not possible for this measure. Figure 14 shows results from a recent study that found dead-end habitats had significantly higher seedstock ($p < 0.05$) than the six other study sites, including main channel sites and the flooded islands of Franks Tract and Mildred Island (Preece et al. 2025). Although other habitat types had less overwintering seedstock than the dead-end habitats, all the habitat types retained *Microcystis* seedstock into the spring. This suggests that multiple locations in the Delta may seed summertime *Microcystis* blooms, but that dead-end habitats contain the highest concentrations. Further work is necessary to fully elucidate the importance of cyanobacteria seedstock as a driver of CHAB formation in the Delta.

https://doi.org/10.15447/sfews.2026v24iss3art?

Remote Sensing

Background

Remote sensing is a useful tool that can be used to estimate phytoplankton biomass over large scales such as in oceans, lakes, and large rivers. This method measures color reflected off the surface of the water via satellite and converts the color to phytoplankton biomass via algorithms. The algorithms were originally developed for sensing ocean color but have since been adapted for freshwater systems. The advantage of using satellite remote sensing is the synoptic view over which data can be acquired. Currently, water color imagery is collected by the Ocean Land Color Instrument (OLCI) sensors onboard the Sentinel-3 satellites (pixel size 300 m x 300 m). The National Oceanic and Atmospheric Administration (NOAA) post processes data from the OLCI sensors to produce a Cyanobacteria Index that estimates cyanobacteria biomass in surface waters. It does so by analyzing wavelengths of light that interact with chl-*a* and phycocyanin (Wynne et al. 2020)

In California, an ocean color visualization tool was adapted for freshwater systems in a partnership between NOAA, the California Surface Water Ambient Monitoring Program (SWAMP), and the San Francisco Estuary Institute (SFEI). The web-based tool to visualize the data, based on using NOAA's CI, is hosted by SFEI.

Delta-Specific Applications

A spatio-temporal analysis of the remote sensing CHAB data for the Delta would be valuable but was outside the scope of this paper. That said, remote sensing is currently very limited in Delta waterways because the current spatial resolution restricts its use to larger water bodies (c.f., > 600 m wide). This excludes many narrow channels and sloughs in the Delta where CHABs most commonly occur. It also excludes areas close to shore (i.e., within 300 m) because the presence of land contaminates the remote-sensing data. Although this tool does not cover most of the narrow Delta waterways it is used to monitor CHABs in the western portion of the Delta, including areas of the Sacramento River, San Joaquin River, Mildred Island, and Franks Tract as well as Clifton Court Forebay. For example, the tool was recently used in the drought year 2021 by Bouma–Gregson et al. (2024) to show a *Dolichospermum* bloom initiating in the southeast side of Franks Tract. This satellite data was especially useful because CHAB monitoring data were limited in Franks Tract, so satellite data were used to fill in monitoring gaps to better understand where the bloom initiated.

Across the broader San Francisco Estuary, satellite imagery has been under-utilized to quantify chl-*a* because of challenges posed by high turbidity, as well as the limited research and funding available to collect the high-resolution observational data necessary for validation. Nonetheless, remote sensing is a rapidly advancing area of study, with research underway to advance the tool so that it can be used for future Delta CHAB monitoring. Of particular relevance to the Delta are efforts to utilize Sentinel-2 satellites, which provide ~15-m spatial resolution at ~5-day intervals, offering more detailed and useful information for Delta waterways.

REGIONAL AND HABITAT ANALYSIS

We examined monthly patterns in the parameters (chl-*a*, microscopy data, total *Microcystis*—cpcB—as measured by qPCR, microcystins, and MVI) across five key regions (CD, LSJR, LSR, SD, and USJR) from June through October. These regions and months were selected because there were data for each parameter for each region during that time-frame. Multivariate differences among months were assessed using PERMANOVA with Bray–Curtis dissimilarities, followed by pairwise PERMANOVA to identify specific month-to-month differences. The overall PERMANOVA indicated a significant effect of month ($R^2 = 0.38$, $p = 0.017$), with pairwise comparisons showing that June conditions were significantly different from July–October ($p < 0.05$). These results provide statistical justification for focusing regional analyses on the July–October period, when CHABs tend to be most severe.

A heatmap was used to visualize relative differences in these parameters across regions. Stockton Waterfront was also added into the analysis to show how a dead-end area differs from the other habitat types. Figure 15 displays the median value of each parameter across regions.

As discussed above, the greatest summertime chl-*a* concentrations occur in the SD, followed by the USJR regions in the Delta (Figure 4). In contrast, the highest frequencies of *Microcystis* detections—particularly of level R5 on the MVI scale—occur in the USJR, followed by the CD and LSJR regions (Figure 9). In other words, there is not a perfect overlap between high chl-*a* concentrations and high *Microcystis* occurrences. One region that stands out in this regard is the SD, where summertime chl-*a* concentrations are frequently not the result of *Microcystis* or other CHAB species. This suggests that the environmental drivers promoting phytoplankton accumulation in general, and CHAB species such as *Microcystis* specifically, may differ somewhat from region to region. Figure 15, along with the individual analysis of parameters above, also highlights how the CSC, ED, and LSR have fewer issues with CHABs than the CD, SD, and USJR. The CSC, LSR and ED rarely, if ever, have microcystin detections (Figures 11 and 12).

Although data for habitat-type comparisons were limited, dead-end habitats exhibited significantly higher microcystin concentrations and overwintering *Microcystis* seedstock than both flooded island and side channels as well as main channel sites. Data for qPCR measurements of *Microcystis* were even more limited by habitat type; however, the heatmap above shows that the median *Microcystis* concentration in dead-end habitats was nearly four times greater than the highest measurement observed in the main channels of the CD, which represented the highest regional values (Figure 15).

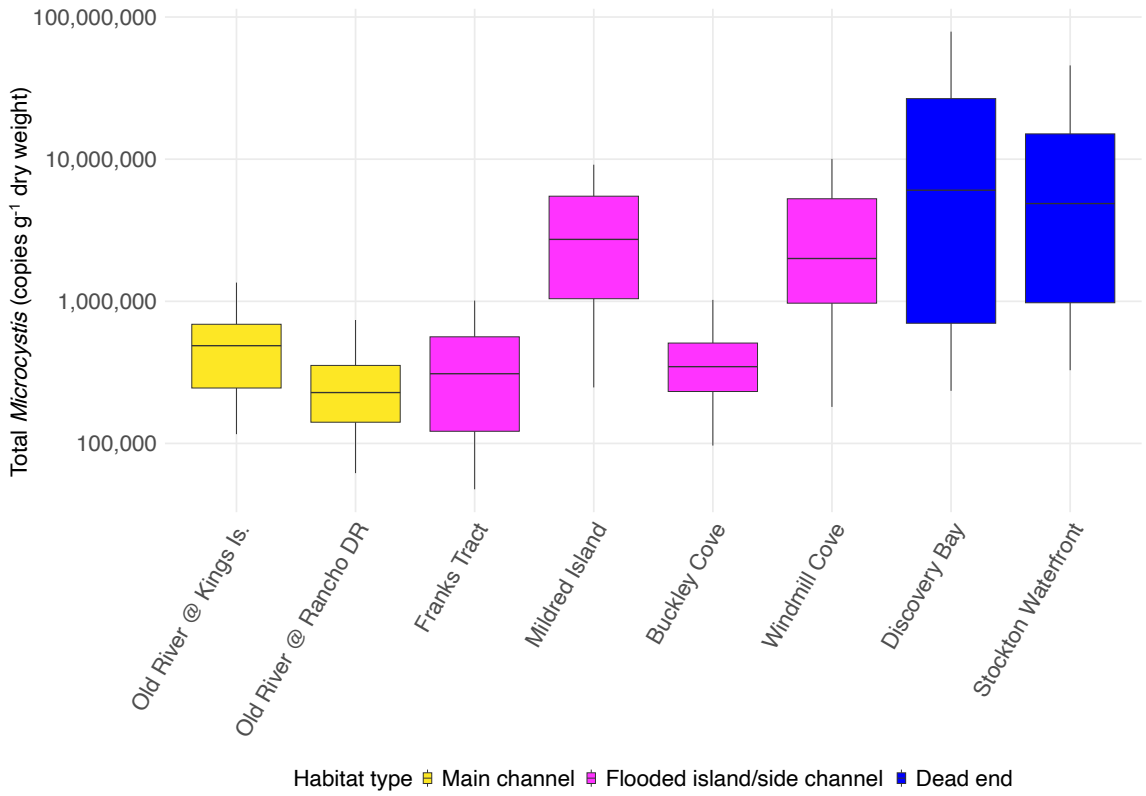

Figure 14 Total *Microcystis* (cpcB cell equivalents) per gram dry sediment measured in April and May 2021 and April 2022 on a log scale. *n* = 10 sediment samples per site Franks Tract *n* = 15, and Discovery Bay in *n* = 15. MC = Main Channel, FI = Flooded Island, OUT = Outlet, and SP = Static Peripheral.

https://doi.org/10.15447/sfews.2026v24iss3art?

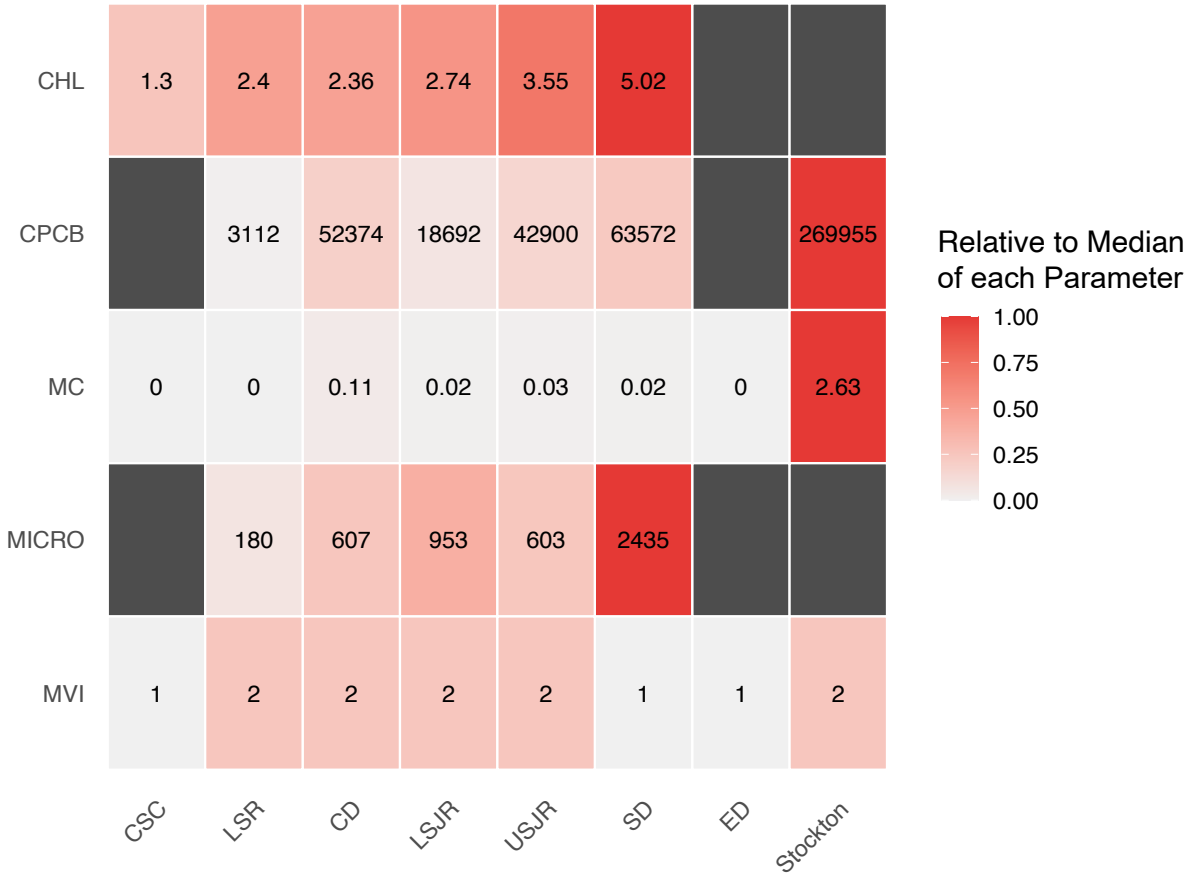

Figure 15 The heatmap shows median values, by parameter, across regions. Median values are shown as numbers within the tiles. *Colors* are scaled separately for each parameter, with the lowest value in the lightest grey shade and the highest in *dark red*; *dark grey* denotes missing data. Because ranges vary, the full color spectrum may not appear for every parameter, and colors are not comparable across different parameters. CHL = chlorophyll-*a*, CPCB = total *Microcystis* measured as gene copies/mL by qPCR, MC = microcystins, MICRO = *Microcystis* cells as detected by microscopy, and MVI = *Microcystis* Visual Index score. CSC = Cache Slough Complex, LSR = lower Sacramento River, CD = Central Delta, LSJR = lower San Joaquin River, USJR = upper San Joaquin River, SD = South Delta, ED = East Delta.

CHAB MONITORING AND RESEARCH CONSIDERATIONS

Here, we have discussed various parameters that are useful for monitoring Delta CHABs, including microscopic enumeration of colony abundances, characterizing colony density using the MVI ranking, using molecular tools as well as remote sensing to detect *Microcystis*, and measuring cyanotoxin concentrations. The data presented herein provide a good starting point for understanding when and where CHABs are problematic in the Delta. One of the biggest challenges in synthesizing Delta CHAB parameters was the temporal and spatial variability among datasets. This made it difficult to compare CHABs across regions and habitat types, but it also uncovered a number of monitoring gaps.

Spatial and Temporal Considerations

For a more complete understanding of CHABs distribution, enhanced monitoring and research should prioritize dead-end channels, such as Discovery Bay, the Stockton Waterfront, and Big Break, as well as similar habitats that remain largely unmonitored. These areas consistently experience the most intense blooms, reaching MVI level R5 and exhibiting the highest microcystin concentrations in the Delta. Data from these sites are currently sporadic, limiting their use for trend analysis

or broader effects on the overall Delta. Chl-*a* and nutrient measurements are especially scarce in these dead-end areas, preventing evaluation of their relationship to *Microcystis* vs. other phytoplankton. Expanding monitoring and research in these CHAB "hotspot" regions would enhance understanding of localized bloom dynamics and provide data critical to guiding targeted mitigation efforts. Moreover, the hotspot areas of Discovery Bay, the Stockton Waterfront, and Big Break are located in or adjacent to areas with high levels of recreational and residential contact, underscoring the public health importance of routine monitoring in these locations. Given the Delta's complex network of channels, other hotspots likely exist in less-visited regions but remain undocumented as a result of limited monitoring coverage. For example, sites such as Tiki Lagoon, Windmill Cove, and Buckley Cove are known to support CHABs but have received little monitoring to date. Identifying and monitoring additional hotspot areas would improve our understanding of Delta CHAB dynamics and associated public health risks.

In addition to focusing monitoring and research efforts on dead-end areas and marinas, monitoring should also be expanded to some flooded islands and side channels, as well as small sloughs. These habitats are highly variable, ranging from large tidal lacustrine areas such as Franks Tract to narrow side channels and sloughs across the Delta. Mildred Island stands out as one location within this habitat type to incorporate into future monitoring. Mildred Island experiences pronounced spatial and temporal variability in currents and mixing, which influences both water- quality conditions and the potential for CHAB development (Monsen et al. 2002). Although the area supports relatively high *Microcystis* seedstock, it has received little targeted CHAB monitoring to date (Preece et al. 2025).

Current Delta monitoring programs focus primarily on main channel sites, where most routine stations are located. However, for parameters such as microcystin concentrations, these sites tend to have fewer detections and lower *Microcystis* seedstock compared to habitat types such as dead-end channels. While continued monitoring at main channel sites remains valuable for tracking long-term trends and assessing CHAB risks under a warming climate, monitoring and special studies in habitats with higher detection rates will be critical for better understanding relationships among parameters. For example, in regions with more frequent CHAB detections, a special study that includes concurrent measurements of microcystin concentrations and *Microcystis* cell abundance could help clarify how biomass and toxin production are related in the Delta. At present, microcystin measurements are rarely collected alongside other CHAB metrics, making it unclear whether the high proportion of non-detects reflects the absence of cells, low biomass below a production threshold, variability among toxin-producing genotypes, or a combination of these factors. Furthermore, the composition of the microcystin dataset, which reflects a mix of routine sampling, incident response, and special studies, may influence detection frequencies among habitat types. Integrating CHAB-specific parameters with environmental data could also provide insight into the Delta conditions that promote toxin production.

Expanded monitoring should also occur in regions with few routine stations, particularly where environmental conditions may support bloom development. Although CHAB data are limited for the ED region, MVI observations indicate the presence of *Microcystis* in the Mokelumne River and its tributaries. Numerous marinas and protected off-channel habitats (e.g., dead-end areas) likely support local *Microcystis* growth and may contribute cells to nearby main channels. This region is not currently monitored for phytoplankton growth or biomass accumulation (e.g., phytoplankton biomass or *Microcystis* abundance), yet it may become increasingly susceptible to CHABs under a warming climate (see Preece et al., this issue). Adding CHAB monitoring in the ED could provide valuable insight into how conditions may transition toward those suitable for bloom development under a warming climate.

https://doi.org/10.15447/sfews.2026v24iss3art?

In the first paper of this series (see Preece et al., this issue), the LSR and CSC were identified as regions with environmental conditions less favorable for CHABs compared to the USJR, CD, and SD, which have higher nutrient concentrations and warmer water temperatures. Here, we confirm using multiple CHAB parameters that the LSR and CSC remain less prone to CHABs and cyanotoxin occurrence than the USJR, CD, and SD. Therefore, prioritizing monitoring in the USJR, CD, SD, as well as expanding into the ED, may provide the greatest insight into CHAB dynamics.

In addition to highlighting habitat types and regions that would benefit from expanded monitoring, our dataset also identifies the seasonal window when CHABs are most likely to occur in the Delta. Temperatures in most locations reach the 19 °C threshold for *Microcystis* initiation by April or May (Lehman et al. 2013; Preece et al., this issue), but elevated MVI scores and microcystin concentrations generally occur from July through October, when temperatures approach the warmer conditions that favor optimal *Microcystis* growth (e.g., You et al. 2018). June detections occur but are largely limited to dead-end channel habitats and regions with a higher proportion of growing areas, such as the CD and USJR, suggesting that bloom initiation in these habitats and regions precedes the broader Delta-wide bloom season. While visible blooms typically decline after October, microcystin concentrations may persist at lower levels later into the season, likely reflecting toxin retained in the water column or sediment after bloom senescence (Bolotaolo et al. 2020). Although qPCR and MVI results indicate that *Microcystis* cells can be present in some regions as early as May, microcystin detections are less common before July across most of the Delta (Figures 9, 11, and 15). These seasonal patterns have direct implications for monitoring design. Collecting data before bloom initiation is valuable for identifying the environmental factors that trigger bloom development. However, if resources are limited, the most effective strategy would be to focus monitoring efforts on the July-through-October window, with monitoring being most important from July through September.

Monitoring and Research Tools

Our findings highlight the need for monitoring approaches that capture both spatial and temporal variability in bloom dynamics. The suite of tools summarized in Table 4 illustrates how multiple methods can be integrated to improve CHAB monitoring and research. Biomass indicators (e.g., chl-*a*, remote sensing, MVI) provide broad-scale coverage, while microscopy and qPCR add taxonomic and genetic resolution. Toxin monitoring through grab samples and SPATT samplers captures short-term fluctuations and time-integrated exposure, emphasizing the value of complementary tools for comprehensive bloom assessment.

Beyond simply expanding monitoring coverage, an effective monitoring and research approach for the Delta should integrate four complementary elements: routine monitoring, targeted research, modeling, and tool development (Sommer et al. 2023). Monitoring provides the foundation for early detection and adaptive response, identifying when and where more detailed sampling or focused investigation is warranted. Targeted research allows testing of specific hypotheses about environmental drivers and bloom mechanisms that cannot be resolved through routine monitoring alone. Modeling offers a framework for exploring system-scale interactions, such as how blooms in "growing areas" may influence adjacent "advective areas," or how environmental conditions modulate bloom persistence. Finally, continued tool development will improve detection capability and spatial resolution. Integrating these elements will create a robust, adaptive framework that advances both understanding and management of Delta CHABs. The following discussion provides examples of how these approaches can be applied to strengthen CHAB monitoring and research in the Delta.

Future use of the MVI may focus on correlating this index more closely with biomass of *Microcystis* sp., as well as cyanotoxin concentrations, and

Table 4 Monitoring tools, the type of information each tool provides, the pros and cons of each tool, and examples of applicability for both management and mitigation

Monitoring tool	Type of information provided	Pros	Cons	Applicability to management	Applicability to mitigation
Chlorophyll-*a*	Indicator of total phytoplankton biomass (photosynthetic pigments).	Easy to collect and analyze; used globally as an indicator of eutrophication; enhances comparability of data with other systems; good for tracking general phytoplankton productivity trends.	Non-specific, cannot distinguish cyanobacteria from other phytoplankton; results can vary with light or nutrient conditions.	Detects trends in phytoplankton biomass; informs adaptive sampling; can be integrated into predictive models.	Early detection of bloom formation to initiate mitigation.
Microscopy	Identifies and counts phytoplankton, including cyanobacterial taxa visually; tracks ecological succession and community shifts over time.	Provides genus-level identification (can identify to species); can detect harmful taxa directly.	Labor-intensive, requires taxonomic expertise; can miss small or rare taxa.	Confirms cyanobacteria presence for targeted management. Supports genera-specific modeling; validates remote sensing or MVI data.	Confirms genera composition to guide species-targeted mitigation such as chemical control.
qPCR (Quantitative Polymerase Chain Reaction)	Detects and quantifies specific cyanobacterial genes or toxin-producing genes.	Highly specific and sensitive; early warning tool for toxin producers.	Requires specialized lab equipment and expertise; does not indicate live vs. dead cells or actual toxin concentration.	Identifies toxic strains to trigger toxin sampling. Tracks trends in toxic populations; informs predictive or risk models; supports species-specific modeling; validates remote sensing and MVI data.	Identifies presence of toxic strains to prioritize targeted toxin reduction or alert systems.
Toxin Measurements	Measures concentrations of cyanotoxins (e.g., microcystins, anatoxin-a, cylindrospermopsin).	Direct measure of potential health risk.	Analytical costs can be high; toxin levels can fluctuate rapidly and may not correlate directly with cell abundance.	Supports posting and health risk decisions. Maps toxin hot-spots; validates models.	Guides targeted mitigation by identifying high-risk areas for toxins.
Grab Samples	Snapshot water samples analyzed for various parameters (cells, toxins, nutrients, etc.).	Simple and widely used.	Limited temporal coverage; may miss short-term events or spatial variability.	Confirms bloom toxicity for rapid response.	Determines toxin hot-spots to guide localized treatment (e.g., aeration, algaecide).
SPATT (Solid Phase Adsorption Toxin Tracking)	Passive sampling of dissolved toxins over time.	Integrates toxin exposure over days to weeks; detects episodic toxin presence.	Does not measure particulate toxins or total concentrations; provides semi-quantitative results. adsorption efficiency varies among resins, complicating use for multiple toxins.	Evaluates chronic exposure and spatial toxin trends. Detects trends over time; identifies persistent or emerging toxin hot-spots.	Monitors effectiveness of long-term mitigation (e.g., nutrient control).
***Microcystis* Visual Index (MVI)**	Visual estimate of *Microcystis* surface scum or bloom intensity.	Rapid, low-cost field indicator; useful for broad spatial surveys.	Subjective; depends on observer's experience and surface conditions.	Triggers adaptive sampling or advisory actions. Tracks temporal and spatial bloom patterns; input for predictive bloom models.	Identifies areas for localized intervention.
Overwintering *Microcystis* Seedstock	Quantifies *Microcystis* cells in bottom sediments that can seed future blooms	Provides insight into bloom initiation potential and spatial hot-spots of re-emergence	Sampling and viability assays are labor-intensive; results may vary with sediment type and overwintering conditions	Informs proactive management strategies, can be used for early-season monitoring, and identifying high-risk regions for future blooms; input for predictive bloom models	Locates high-risk sediment areas for dredging, sediment capping, or nutrient removal to reduce bloom initiation
Remote Sensing	Satellite or drone-based estimation of algal pigments, bloom extent, and distribution	Broad spatial coverage; useful for trend detection and mapping	Limited by cloud cover, water depth, shoreline land interference, and sensor resolution; may require ground-truthing	Guides sampling priorities and public outreach; identifies spatial hot-spots; evaluates system-wide bloom trends; informs large-scale management planning; integrates into predictive models for early-season bloom risk	Identifies spatial bloom extent to prioritize mitigation interventions (e.g., nutrient reduction in source areas, targeted mixing)

https://doi.org/10.15447/sfews.2026v24iss3art?

streamlining the measurement to minimize observer bias. Collecting these parameters together in a coordinated manner would allow for targeted research to evaluate how MVI rankings correspond to bloom magnitude and toxicity, providing a stronger scientific basis for interpreting field observations. Integrating such paired measurements into the existing Eulerian monitoring framework in key areas could improve CHAB monitoring, and the understanding of CHAB drivers. Beyond refining existing tools such as the MVI, combining methods in novel ways (e.g., integrating imaging and molecular tools) could also strengthen connections between monitoring and process-level understanding across different habitat types and regions of the Delta. With the addition of CHAB-specific parameters to the existing environmental driver monitoring framework, models can be developed to predict and better understand future CHAB occurrences. These modeling approaches can, in turn, identify where additional data collection would be most beneficial, which can guide targeted monitoring enhancements and ensure that research and management efforts remain closely aligned.

While MVI is cost-effective, it do not directly measure cyanotoxins, which are of primary concern for human, animal, and ecosystem health. Grab sampling is resource-intensive and yields data that are spatially and temporally constrained. To more effectively characterize cyanotoxin occurrence and distribution across the Delta, greater integration of other tools into monitoring frameworks is warranted. One promising approach is the use of SPATT samplers (e.g., Roué et al. 2018; Pindihama et al. 2023). Delta- specific SPATT protocols should include a broader suite of cyanotoxins and emphasize deployment at strategically selected sites that capture habitat heterogeneity—with priority given to areas with a history of elevated toxin production. Further, deployment length and resin type should be standardized among Delta monitoring programs. In particular, placement of SPATT samplers at Banks Pumping Plant, a downstream location that integrates much of the Delta's water, as well as at sites near the confluence of the Sacramento and San Joaquin rivers, would provide valuable system-integrated measurements of multiple toxins. This information is valuable for understanding ecological effects in the Delta and may reveal trends in microcystin concentrations while also improving detection of other cyanotoxins.

The incorporation of molecular tools, such as qPCR and high-throughput sequencing (DNA metabarcoding), could unify disparate datasets if common PCR primers are chosen. For example, the Earth Microbiome Project encourages the use of universal 16S rRNA primers that enable datasets generated from all environments and locations to be compared directly across studies and environments. Currently lacking is a formal bioinformatic pipeline and reference database in which all researchers generating sequencing data could create complementary datasets (Bailet et al. 2020). For qPCR, if the same assays and assay conditions are used, then the same results in the form of gene copies per volume should be reproducible by any laboratory experienced in the method. These advantages become particularly apparent when compared to traditional microscopy which, although the standard for hundreds of years, suffers from quantification bias (e.g., over-estimation of high biovolume species), observer bias (personal experience), and a propensity to miss or misidentify very small-celled taxa such as picocyanobacteria (c.f., MacKeigan et al. 2022). This highlights the importance of continued methodological research and development—an example of targeted research—to improve data comparability and reliability.

One example of ongoing tool development is the advancement of remote-sensing applications for CHAB monitoring in the Delta. While remote sensing offers considerable potential for CHAB monitoring in the Delta, current products such as the Cyanobacterial Index are limited by coarse resolution (300 m) and have not yet been evaluated for status and trends. Ongoing efforts to apply higher-resolution Sentinel-2 imagery (~15 m every 5 days) suggest that remote sensing will become an increasingly important tool for tracking

CHABs in Delta waterways. Use of Sentinel-2 satellite imagery could offer the most effective means of identifying additional bloom hotspots across the Delta.

Linking monitoring data to management and mitigation actions is critical to ensure that the information collected translates into meaningful outcomes (Table 4). The approaches proposed here—ranging from image-based assessments and toxin measurements to monitoring overwintering *Microcystis* seedstock—can each inform distinct management decisions operating across different spatial and temporal scales. For example, near-real-time indicators such as chl-*a* and MVI classifications can be used to trigger adaptive sampling, while toxin measurements provide quantitative information to support decisions related to bloom severity, exposure risk, and public notification. Overwintering seedstock assessments and nutrient data can guide longer-term management strategies, such as identifying sediment-removal targets or prioritizing nutrient-reduction efforts. Together, these examples demonstrate how integrating monitoring, targeted research, modeling, and tool development into a decision-based framework ensures that resulting datasets are actionable, supporting timely responses and adaptive management to mitigate the effect of blooms in the Delta.

CONCLUSION

The Delta is a hydrologically complex system with large regional variation in the occurrence of CHABs. In this study, we confirm across multiple CHAB parameters that the LSR and CSC regions remain less prone to CHABs and cyanotoxin occurrence than the USJR, CD, and SD regions. Therefore, prioritizing monitoring in the USJR, CD, and SD—as well as enhanced monitoring efforts in the ED—may provide the greatest insight into CHAB dynamics. In addition, focusing monitoring efforts on the July-through-October window may be the most economical and efficient. Concurrent measurements of CHAB biomass, toxin concentrations, and environmental drivers may yield important insights into bloom dynamics specific to the Delta. Finally, including sediment seedstock measurements helps quantify bloom initiation potential across regions and where risks of future occurrences are greatest. Sediment seedstock measurements could also be a valuable tool to investigate whether CHAB mitigation measures—including dredging, oxygenation, and/or chemical applications—are successful.

Climate-induced changes are expected to exacerbate CHAB issues in many water bodies across the world, including in the Delta. Further, ongoing human modifications to the system will continue to intensify pressures on ecosystem health and management. In the Delta, management solutions will need to evolve to ensure delivery of clean fresh water to central and southern California. The addition of management interventions, such as salinity barriers or gates, on top of extreme drought conditions may further promote CHABs in certain areas of the Delta (Bosworth et al. 2024; Bouma–Gregson et al. 2024). This underscores the need for managers and scientists to anticipate such conditions and develop innovative, adaptive strategies to address the growing challenges posed by climate change and associated CHAB proliferation.

ACKNOWLEDGEMENTS

This paper was made possible by the foundation laid in the Cyanobacteria Harmful Algal Bloom Monitoring Strategy for the Sacramento–San Joaquin Delta. We are grateful to the many individuals who contributed to the writing and review of that strategy; their collective effort provided the vision and framework on which this work is based. We also thank the Environmental Monitoring Program, the Biogeochemistry Group at the USGS California Water Science Center, Restore the Delta, and East Bay Regional Parks for providing essential data. Special thanks to Jereme Gaeta for his guidance with statistical analyses and to Travis Hinkelman for developing the *Microcystis* Visual Index R Shiny App. We further acknowledge Janis Cooke, Dave Bosworth, Rosemary Hartman, Emily Richardson, and Jenna Rinde for their thoughtful insights and review of this manuscript. We thank the Delta

Stewardship Council for graphic design and production of Figure 1; the conceptual design and content were developed by the authors. The purpose of this paper is to examine how CHAB occurrence varies across Delta regions and habitat types using historical monitoring data, with the goal of improving future monitoring and research efforts. The findings presented here likely stem from the combined effects of current and historical watershed uses and changing environmental conditions. Views expressed in this paper are those of authors and not the California Department of Water Resources.

REFERENCES

Bailet B, Apothéloz–Perret–Gentil L, Baričević A, Chonova T, Franc A, Frigerico J–M, Kelly M, Mara D, Pfannkuchen M, Proft S, et al. 2020. Diatom DNA metabarcoding for ecological assessment: comparison among bioinformatics pipelines used in six European countries reveals the need for standardization. Sci Total Environ. [accessed 2026 Jun 27];745:140948. *https://doi.org/10.1016/j.scitotenv.2020.140948*

Berg M, Sutula M. 2015. Factors affecting the growth of cyanobacteria with special emphasis on the Sacramento–San Joaquin Delta. Southern California Coastal Water Research Project Technical Report 869. Costa Mesa (CA): Southern California Coastal Water Research Project. [accessed 2026 Jun 27]. 111 p. Available from: *https://amarine.com/wp-content/uploads/2018/01/Cyano_Review_Final.pdf*

Bertone E, Burford MA, Hamilton DP. 2018. Fluorescence probes for real-time remote cyanobacteria monitoring: a review of challenges and opportunities. Water Res. [accessed 2026 Jun 27];141:152–162. *https://doi.org/10.1016/j.watres.2018.05.001*

Bolotaolo M, Kurobe T, Puschner B, Hammock BG, Hengel MJ, Lesmeister S, Teh SJ. 2020. Analysis of covalently bound microcystins in sediments and clam tissue in the Sacramento–San Joaquin River Delta, California, USA. Toxins. [accessed 2026 Jun 27];12(3):178. *https://doi.org/10.3390/toxins12030178*

Bosworth DH, Bashevkin SM, Bouma–Gregson K, Hartman R, Stumpner EB. 2024. The anatomy of a drought in the upper San Francisco Estuary: water quality and lower-trophic responses to multi-year droughts over a long-term record (1975–2021). San Franc Estuary Watershed Sci. [accessed 2026 Jun 27];22(1). *https://doi.org/10.15447/sfews.2024v22iss1art1*

Bouma–Gregson K, Bosworth DH, Flynn TM, Maguire A, Rinde J, Hartman R. 2024. Delta blue(green)s: the effect of drought and drought-management actions on *Microcystis* in the Sacramento–San Joaquin Delta. San Franc Estuary Watershed Sci. [accessed 2026 Jun 27];22(1). *https://doi.org/10.15447/sfews.2024v22iss1art2*

Bouma–Gregson K, Sturgeon CL, Cone KM, Uebner MQ, Baxter TJ, Nakatsuka KK, Hansen AM, Richardson ET, Westrick J, Szlag Silva R, et al. 2025. Cyanotoxins in the California Sacramento–San Joaquin Delta: fixed station solid phase adsorption toxin tracking (SPATT) samplers. Reston (VA): US Geological Survey. Dataset. [accessed 2026 Jun 27]. *https://doi.org/10.5066/P13ZCBI5*

Cai P, Cai Q, He F, Huang Y, Tian C, Wu X, Wang C, Xiao B. 2021. Flexibility of Microcystis overwintering strategy in response to winter temperatures. Microorganisms. [accessed 2026 Jun 27];9(11):2278. *https://doi.org/10.3390/microorganisms9112278*

Caporaso JG, Lauber CL, Walters WA, Berg–Lyons D, Lozupone CA, Turnbaugh PJ, Fierer N, Knight R. 2010. Global patterns of 16S rRNA diversity at a depth of millions of sequences per sample. Proc Natl Acad Sci. [accessed 2026 Jun 27];108:4516–4522. *https://doi.org/10.1073/pnas.1000080107*

Carmichael WW. 1992. Cyanobacteria secondary metabolites—the cyanotoxins. J Appl Bacteriol. [accessed 2026 Jun 27];72(6):445–459. *https://doi.org/10.1111/j.1365-2672.1992.tb01858.x*

[CDC] Centers for Disease Control and Prevention. c2021. Centers for Disease Control and Prevention, National Center for Environmental Health. 2026. Environmental Public Health Practices Gateway: Harmful algal bloom monitoring in recreational and drinking water. A practice from Tracking California, a program of the Public Health Institute. Atlanta (GA): U.S. Department of Health and Human Services, CDC. [accessed 2026 Aug 27]. *https://www.cdc.gov/environmental-health-practice/php/gateway/harmful-algal-bloom-monitoring-in-recreational-and-drinking-water.html*

[CDEC] California Data Exchange Center. 2024. Chronological reconstructed Sacramento and San Joaquin Valley water year hydrologic classification indices. [accessed 2026 Jun 27]. Available from: *https://cdec.water.ca.gov/reportapp/javareports?name=WSIHIST*

Cheung MY, Liang S, Lee J. 2013. Toxin-producing cyanobacteria in freshwater: a review of the problems, impact on drinking water safety, and efforts for protecting public health. J Microbiol. [accessed 2026 Jun 27];51(1):1–10. *https://doi.org/10.1007/s12275-013-2549-3*

Chorus I, Welker M. 2021. Cyanobacterial toxins. In: Chorus I, Welker M, editors. Toxic cyanobacteria in water. 2nd ed. Boca Raton (FL): CRC Press. p. 13–162. Available from: *https://www.who.int/publications/m/item/toxic-cyanobacteria-in-water---second-edition*

Cloern JE, Foster SQ, Kleckner AE. 2014. Phytoplankton primary production in the world's estuarine–coastal ecosystems. Biogeosciences. [accessed 2026 Jun 27];11:2477–2501. *https://doi.org/10.5194/bg-11-2477-2014*

Cloern JE, Jassby AD. 2012. Drivers of change in estuarine–coastal ecosystems: discoveries from four decades of study in San Francisco Bay. Rev Geophys. [accessed 2026 Jun 27];50(4):RG4001. *https://doi.org/10.1029/2012RG000397*

[CWQMC] California Water Quality Monitoring Council. 2026. Standard operating procedures: water sample collection for toxin analysis for surface water samples (planktonic blooms). [accessed 2026 Jun 27]. Sacramento (CA): California State Water Resources Control Board. 9 p. Available from: *https://mywaterquality.ca.gov/habs/docs/sample-collection-for-toxin-analysis.pdf*

Dodds WK, Bouska WW, Eitzmann JL, Pilger TJ, Pitts KL, Riley AJ, Schloesser JT, Thornbrugh DJ. 2009. Eutrophication of US freshwaters: analysis of potential economic damages. Environ Sci Technol. [accessed 2026 Jun 27];43:12–19. *https://doi.org/10.1021/es801217q*

Flynn T, Lehman P, Lesmeister S, Waller S. 2022. A visual scale for *Microcystis* bloom severity. figshare. Figure. [accessed 2026 Jun 27]. *https://doi.org/10.6084/m9.figshare.19239882.v1*

Gowen RJ, Tett P, Jones KJ. 1992. Predicting marine eutrophication: the yield of chlorophyll from nitrogen in Scottish coastal waters. Mar Ecol Prog Ser. [accessed 2026 Jun 27];85:153–161. *https://doi.org/10.3354/meps085153*

Gupta S, Gupta S. 2025. Time series forecasting of chlorophyll-a concentrations in the Chesapeake Bay. Sci Rep. [accessed 2026 Jun 27];15(1):30877. *https://doi.org/10.1038/s41598-025-16352-3*

Harke MJ, Steffen MM, Gobler CJ, Otten TG, Wilhelm SW, Wood SA, Paerl HW. 2016. A review of the global ecology, genomics, and biogeography of the toxic cyanobacterium *Microcystis* spp. Harmful Algae. [accessed 2026 Jun 27];54:4–20. Available from: *https://repository.library.noaa.gov/view/noaa/48450*

Hartman R, Stumpner EB, Bosworth DH, Maguire A, Burdi CE, Drought Synthesis Team, Interagency Ecological Program. 2024. Dry me a river: ecological effects of drought in the upper San Francisco Estuary. San Franc Estuary Watershed Sci. [accessed 2026 Jun 27];22(1). *https://doi.org/10.15447/sfews.2024v22iss1art5*

Havens KE. 2008. Cyanobacteria blooms: effects on aquatic ecosystems. In: Hudnell HK, editor. Cyanobacterial harmful algal blooms: state of the science and research needs. New York (NY): Springer. p. 733–747. Available from: *https://link.springer.com/chapter/10.1007/978-0-387-75865-7_33*

Hooker SB, Van Heukelem L. 2011. An investigation into HPLC data quality problems. NASA/ TP -2011-215867. Greenbelt (MD): NASA Goddard Space Flight Center. [accessed 2026 Jun 27]. 50 p. Available from: *https://oceancolor.gsfc.nasa.gov/fsg/hplc/chors-hplc/Hooker-215867-S.pdf*

Howard MDA, Nagoda C, Kudela RM, Hayashi K, Tatters A, Caron DA, Busse L, Brown J, Sutula M, Stein ED. 2017. Microcystin prevalence throughout lentic waterbodies in coastal southern California. Toxins. [accessed 2026 Jun 27];9(7):231. *https://doi.org/10.3390/toxins9070231*

Howard MDA, Smith J, Caron DA, Kudela RM, Loftin K, Hayashi K, Fadness R, Fricke S, Kann J, Roethler M, et al. 2023. Integrative monitoring strategy for marine and freshwater harmful algal blooms and toxins across the freshwater-to-marine continuum. Integr Environ Assess Manag. [accessed 2026 Jun 27];19(3):586–604. *https://doi.org/10.1002/ieam.4651*

Humphries SE, Lyne VD. 1988. Cyanophyte blooms: the role of cell buoyancy. Limnol Oceanogr. [accessed 2026 Jun 27];33(1):79–91. *https://doi.org/10.4319/lo.1988.33.1.0079*

Jassby AD, Cloern JE, Cole BE. 2002. Annual primary production: patterns and mechanisms of change in a nutrient-rich tidal ecosystem. Limnol Oceanogr. [accessed 2026 Jun 27];47:698–712. *https://doi.org/10.4319/lo.2002.47.3.0698*

Jassby AD, Kimmerer WJ, Monismith SG, Armor C, Cloern JE, Powell TM, Schubel JR, Vendlinski TJ. 1995. Isohaline position as a habitat indicator for estuarine populations. Ecol Appl. [accessed 2026 Jun 27];5:272–289. *https://doi.org/10.2307/1942069*

Jeffrey SW, Wright S, Zapata M. 2011. Microalgal classes and their signature pigments. In: Phytoplankton pigments: characterization, chemotaxonomy and applications in oceanography. Cambridge (UK): Cambridge University Press. [accessed 2026 Jun 27]. p 3–77. Available from: *https://hdl.handle.net/102.100.100/535302*

Jungbluth M, Lee C, Patel C, Ignoffo T, Bergamaschi B, Kimmerer W. 2021. Production of the copepod *Pseudodiaptomus forbesi* is not enhanced by ingestion of the diatom *Aulacoseira granulata* during a bloom. Estuaries Coasts. [accessed 2026 Jun 27];44(4):1083–1099. *https://doi.org/10.1007/s12237-020-00843-9*

Kimmerer WJ. 2004. Open water processes of the San Francisco Estuary: from physical forcing to biological responses. San Franc Estuary Watershed Sci. [accessed 2026 Jun 27];2(1). *https://escholarship.org/uc/item/9bp499mv*

Kimmerer W, Ignoffo TR, Bemowski B, Modéran J, Holmes A, Bergamaschi B. 2018. Zooplankton dynamics in the Cache Slough complex of the upper San Francisco Estuary. San Francisco Estuary Watershed Sci. [accessed 2026 Jun 27];16(3). *https://doi.org/10.15447/sfews.2018v16iss3art4*

Kimmerer W, Wilkerson F, Downing B, Dugdale R, Gross ES, Kayfetz K, Shruti K, Parker AE, Thompson J. 2019. Effects of drought and the emergency drought barrier on the ecosystem of the California Delta. San Francisco Estuary and Watershed Science. [accessed 2026 Jun 27]; 17(3). *https://doi.org/10.15447/sfews.2019v17iss3art2*

Kopfmann S, Roesch SK, Hess WR. 2016. Type II toxin–antitoxin systems in the unicellular cyanobacterium *Synechocystis* sp. PCC 6803. Toxins. [accessed 2026 Jun 27];8(7):228. *https://doi.org/10.3390/toxins8070228*

Kramer SJ, Siegel DA, Maritorena S, Catlett D. 2022. Modeling surface ocean phytoplankton pigments from hyperspectral remote sensing reflectance on global scales. Remote Sens Environ. [accessed 2026 Jun 27];270:112879. *https://doi.org/10.1016/j.rse.2021.112879*

Kudela RM. 2011. Characterization and deployment of solid phase adsorption toxin tracking (SPATT) resin for monitoring of microcystins in fresh and saltwater. Harmful Algae. [accessed 2026 Jun 27];11:117–125. *https://doi.org/10.1016/j.hal.2011.08.006*

Kudela RM. 2017. Passive sampling for freshwater and marine algal toxins. In: Diogene J, Campas, editors. Recent advances in the analysis of marine toxins. Comprehensive analytical chemistry. Vol. 78. Amsterdam (Netherlands): Elsevier. p. 379–409.

Kudela RM, Howard MDA, Monismith S, Paerl HW. 2023. Status, trends, and drivers of harmful algal blooms along the freshwater to marine gradient in the San Francisco Bay–Delta system. San Franc Estuary Watershed Sci. [accessed 2026 Jun 27];20(4). *https://doi.org/10.15447/sfews.2023v20iss4art6*

Kurobe T, Lehman PW, Lesmeister S, Teh SJ. 2022. Cyanobacteria abundance, cyanotoxin concentration, and water quality data for the upper San Francisco Estuary, California, USA: 2014–2019. Environmental Data Initiative. [accessed 2026 Jun 27]. *https://doi.org/10.6073/pasta/b4e180cb925266171285375a3e202635*

Le VV, Srivastava A, Ko S–R, Ahn C–Y, Oh H–M. 2022. *Microcystis* colony formation: extracellular polymeric substance, associated microorganisms, and its application. Bioresour Technol. [accessed 2026 Jun 27];360:127610. *https://doi.org/10.1016/j.biortech.2022.127610*

Lehman PW, Marr K, Boyer GL, Acuna S, Teh SJ. 2013. Long-term trends and causal factors associated with Microcystis abundance and toxicity in San Francisco Estuary and implications for climate change impacts. Hydrobiologia. [accessed 2026 Aug 27];718:141–158. *https://doi.org/10.1007/s10750-013-1612-8*

Lehman P. 2022. The increase of cyanobacteria and benthic diatoms over 43 years in upper San Francisco Estuary, California. Estuarine Coast Shelf Sci. [accessed 2026 Jun 27];275:107988. *https://doi.org/10.1016/j.ecss.2022.107988*

Lehman PW, Boyer G, Hall C, Waller S, Gehrts K. 2005. Distribution and toxicity of a new colonial *Microcystis aeruginosa* bloom in the San Francisco Bay Estuary, California. Hydrobiologia. [accessed 2026 Jun 27];541(1):87–99. *https://doi.org/10.1007/s10750-004-4670-0*

Lehman PW, Boyer G, Satchwell M, Waller S. 2008. The influence of environmental conditions on the seasonal variation of *Microcystis* cell density and microcystins concentration in San Francisco Estuary. Hydrobiologia. [accessed 2026 Jun 27];600:187–204. *https://doi.org/10.1007/s10750-007-9231-x*

Lehman PW, Kendall C, Guerin MA, Young MB, Silva SR, Boyer GL, Teh SJ. 2015. Characterization of the *Microcystis* bloom and its nitrogen supply in San Francisco Estuary using stable isotopes. Estuaries Coasts. [accessed 2026 Jun 27];38:165–178. *https://doi.org/10.1007/s12237-014-9811-8*

Lehman PW, Kurobe T, Lesmeister S, Baxa D, Tung A, Teh SJ. 2017. Impacts of the 2014 severe drought on the *Microcystis* bloom in San Francisco Estuary. Harmful Algae. [accessed 2026 Jun 27];63:94–108. *https://doi.org/10.1016/j.hal.2017.01.011*

Lehman PW, Kurobe T, Teh SJ. 2022. Impact of extreme wet and dry years on the persistence of Microcystis harmful algal blooms in San Francisco Estuary. Quat Int. [accessed 2026 Jun 27];621:16–25. *https://doi.org/10.1016/j.quaint.2019.12.003*

Lehman PW, Teh SJ, Boyer GL, Nobriga ML, Bass E, Hogle C. 2010. Initial impacts of *Microcystis aeruginosa* blooms on the aquatic food web in the San Francisco Estuary. Hydrobiologia. [accessed 2026 Jun 27];637(1):229–248. *https://doi.org/10.1007/s10750-009-9999-y*

Loaiza–González JM, Rubio–Clemente A, Peñuela GA. 2024. Cyanotoxin monitoring and detection using passive sampling application. Water Air Soil Pollut. [accessed 2026 Jun 27];235(7):423. *https://doi.org/10.1007/s11270-024-07195-1*

Lopez C, Cloern JE, Schraga TS, Little AJ, Lucas LV, Thompson JK, Burau JR. 2006. Ecological values of shallow-water habitats: implications for the restoration of disturbed ecosystems. Ecosystems. [accessed 2026 Jun 27];9:422–440. *https://doi.org/10.1007/s10021-005-0113-7*

Lucas LV, Cloern JE, Thompson JK, Monsen NE. 2002. Functional variability of habitats within the Sacramento–San Joaquin Delta: restoration implications. Ecol Appl. [accessed 2026 Jun 27];12(5):1528–1547. *https://doi.org/10.1890/1051-0761(2002)012[1528:FVOHWT]2.0.CO;2*

Ma L, Moradinejad S, Guerra Maldonado JF, Zamyadi A, Dorner S, Prévost M. 2022. Factors affecting the interpretation of online phycocyanin fluorescence to manage cyanobacteria in drinking water sources. Water. [accessed 2026 Jun 27];14(22):3749. *https://doi.org/10.3390/w14223749*

MacKeigan PW, Garner RE, Monchamp MÈ, Walsh DA, Onana VE, Kraemer SA, Pick FR, Beisner BE, Agbeti MD, Barbosa de Costa N, et al. 2022. Comparing microscopy and DNA metabarcoding techniques for identifying cyanobacteria assemblages across hundreds of lakes. Harmful Algae. [accessed 2026 Jun 27];113:102187. *https://doi.org/10.1016/j.hal.2022.102187*

Mackey MD, Mackey DJ, Higgins HW, Wright SW. 1996. CHEMTAX: a program for estimating class abundances from chemical markers: application to HPLC measurements of phytoplankton. Mar Ecol Prog Ser. [accessed 2026 Jun 27];144:265–283. *https://doi.org/10.3354/meps144265*

Miller MA, Kudela RM, Mekebri A, Crane D, Oates SC, Tinker MT, Staedler M, Miller WA, Toy–Choutka S, Dominik C, et al. 2010. Evidence for a novel marine harmful algal bloom: cyanotoxin (microcystin) transfer from land to sea otters. PLoS ONE. [accessed 2026 Jun 27];5(9):e12576. *https://doi.org/10.1371/journal.pone.0012576*

Mioni C, Kudela R, Baxa D, Sullivan M, Hayashi K, Smythe T, White C, Waller S, Sakata B, Kurobe T, et al. 2011. Harmful cyanobacteria blooms and their toxins in Clear Lake and the Sacramento–San Joaquin Delta (California). [accessed 2026 Jun 27]. Prepared for the California Regional Water Quality Control Board under the auspices of Surface Water Ambient Monitoring Program (SWAMP). Report #10-058-150. 110 p. Available from: *https://www.researchgate.net/profile/Dolores-Baxa/publication/276204783_Harmful_cyanobacteria_blooms_and_their_toxins_in_Clear_Lake_and_the_Sacramento-San_Joaquin_Delta_California/links/5552269108ae6943a86d6e2a/Harmful-cyanobacteria-blooms-and-their-toxins-in-Clear-Lake-and-the-Sacramento-San-Joaquin-Delta-California.pdf*

Monsen NE, Cloern JE, Lucas LV, Monismith SG. 2002. A comment on the use of flushing time, residence time, and age as transport time scales. Limnol Oceanogr. [accessed 2026 Jun 27];47(5):1545–1553. *https://doi.org/10.4319/lo.2002.47.5.1545*

Moreira C, Ramos V, Azevedo J, Vasconcelos V. 2014. Methods to detect cyanobacteria and their toxins in the environment. Appl Microbiol Biotechnol. [accessed 2026 Jun 27];98:8073–8082. *https://doi.org/10.1007/s00253-014-5951-9*

Moreira C, Vasconcelos V, Antunes A. 2022. Cyanobacterial blooms: current knowledge and new perspectives. Earth. [accessed 2026 Jun 27];3(1):127–135. *https://doi.org/10.3390/earth3010010*

Mussen TD, Driscoll S, Cook ME, Nordin JD, Guerin M, Rachiele R, Smith DJ, Mine Berg G, Thompson LC. 2023. Investigating factors contributing to phytoplankton biomass declines in the lower Sacramento River. San Franc Estuary Watershed Sci. [accessed 2026 Jun 27];21(1). *https://doi.org/10.15447/sfews.2023v21iss1art3*

Neilan BA, Jacobs D, Goodman AE. 1995. Genetic diversity and phylogeny of toxic cyanobacteria determined by DNA polymorphisms within the phycocyanin locus. Appl Environ Microbiol. [accessed 2026 Jun 27];61(11):3875–3883. *https://doi.org/10.1128/aem.61.11.3875-3883.1995*

Nixon SW. 1995. Coastal marine eutrophication: a definition, social causes, and future concerns. Ophelia. [accessed 2026 Jun 27];41(1):199–219. *https://doi.org/10.1080/00785236.1995.10422044*

Oksanen J, Simpson G, Blanchet F, Kindt R, Legendre P, Minchin P, O'Hara R, Solymos P, Stevens M, Szoecs E, et al. 2025. vegan: Community Ecology Package. R package version 2.8-0. [accessed 2026 Jun 27]. Available from: *https://vegandevs.github.io/vegan/*

Otten TG, Mackey S, Crosswell JR, Dreher TG. 2015. Application of molecular tools for microbial source tracking and public health risk assessment of a *Microcystis* bloom traversing 300 km of the Klamath River. Harmful Algae. [accessed 2026 Jun 27];46:71–81. *https://doi.org/10.1016/j.hal.2015.05.007*

Otten TG, Paerl HW, Dreher TW, Kimmerer WJ, Parker AE. 2017. The molecular ecology of *Microcystis* sp. blooms in the San Francisco Estuary. Environ Microbiol. [accessed 2026 Jun 27];19(9):3619–3637. *https://doi.org/10.1111/1462-2920.13860*

Peacock MB, Gibble CM, Senn DB, Cloern JE, Kudela RM. 2018. Blurred lines: multiple freshwater and marine algal toxins at the land–sea interface of San Francisco Bay, California. Harmful Algae. [accessed 2026 Jun 27];73:138–147. *https://doi.org/10.1016/j.hal.2018.02.005*

Perry SE, Brown T, Klotz V. 2023. Interagency Ecological Program: Phytoplankton monitoring in the Sacramento–San Joaquin Bay Delta, collected by the Environmental Monitoring Program, 2008–2022. Environmental Data Initiative. [accessed 2026 Jun 27]. *https://doi.org/10.6073/pasta/e7f0c91851ab2c5f41a05dfb69bd32d1*

Phlips EJ, Badylak S, Milbrandt EC, Stelling B, Arias M, Armstrong C, Behlmer T, Chappel A, Foss A, Kaplan D, et al. 2025. Fate of a toxic *Microcystis aeruginosa* bloom introduced into a subtropical estuary from a flow managed canal and management implications. J Environ Manag. [accessed 2026 Jun 27];375:124362. *https://doi.org/10.1016/j.jenvman.2025.124362*

Pindihama GK, Gitari WM, Mukangaya S. 2023. Application of solid phase adsorption toxin tracking technology (SPATT) for monitoring microcystins in farm dams in Levubu farming area, South Africa. Phys Chem Earth. [accessed 2026 Jun 27];132:103500. *https://doi.org/10.1016/j.pce.2023.103500*

Preece EP, Berg M, Lee T, Odkins K, Rinder J. 2024. Cyanobacteria harmful algal bloom monitoring strategy for the Sacramento–San Joaquin Delta. [accessed 2026 Jun 27]. Sacramento (CA): Delta Stewardship Council, Delta Science Program. 150 p. Available from: *https://deltacouncil.ca.gov/pdf/science-program/2024-10-21-final-delta-chabs-monitoring-strategy.pdf*

Preece EP, Hardy FJ, Moore BC, Bryan M. 2017. A review of microcystin detections in estuarine and marine waters: environmental implications and human health risk. Harmful Algae. [accessed 2026 Jun 27];61:31–45. *https://doi.org/10.1016/j.hal.2016.11.006*

Preece EP, Otten TG, Cooke J. 2024. Use of multiple sampling techniques for cyanobacteria and cyanotoxin monitoring in the Sacramento–San Joaquin Delta under different hydrologic regimes. Mar Pollut Bull. [accessed 2026 Jun 27];205:116585. *https://doi.org/10.1016/j.marpolbul.2024.116585*

Preece EP, Otten TG, Cooke J, Cook KV. 2025. Role of benthic overwintering cyanobacteria seed stock on estuarine bloom dynamics. Harmful Algae. [accessed 2026 Jun 27];143:102807. *https://doi.org/10.1016/j.hal.2025.102807*

Preece EP, Otten TG, Cooke J, Kudela RM. 2024. Microcystin in the benthic food web of the Sacramento–San Joaquin Delta, California. Sci Total Environ. [accessed 2026 Jun 27];946:174250. *https://doi.org/10.1016/j.scitotenv.2024.174250*

R Core Team. 2025. The R project for statistical computing. [accessed 2026 Jun 27]. Vienna (Austria): R foundation for statistical computing. Available from: *https://www.R-project.org/*

Reynolds CS. 1994. The long, the short and the stalled: on the attributes of phytoplankton selected by physical mixing in lakes and rivers. Hydrobiologia. [accessed 2026 Jun 27];289(1):9–21. *https://doi.org/10.1007/BF00007405*

Richardson ET, Bouma–Gregson K, Kraus TEC, O'Donnell K, Sturgeon CL, Soto Perez J, Delascagigas A, Nakatsuka KK, Burau DJ, Gelber AD, et al. 2023. Phytoplankton species composition and abundance in the Sacramento–San Joaquin River Delta: microscopic enumeration of USGS samples, beginning in 2016. (Version 1.1, December 2023). [accessed 2026 Jun 27]. Reston (VA): US Geological Survey. Dataset. Available from: *https://doi.org/10.5066/P97ZBPLH*

Roué M, Darius HT, Chinain M. 2018. Solid phase adsorption toxin tracking (SPATT) technology for the monitoring of aquatic toxins: a review. Toxins. [accessed 2026 Jun 27];10(4):167. *https://doi.org/10.3390/toxins10040167*

Rousso BZ, Bertone E, Stewart R, Aguiar A, Chuang A, Hamilton DP, Burford MA. 2022. Chlorophyll and phycocyanin in situ fluorescence in mixed cyanobacterial species assemblages: effects of morphology, cell size and growth phase. Water Res. [accessed 2026 Jun 27];212:118127. *https://doi.org/10.1016/j.watres.2022.118127*

Sommer T, Conrad JL, Culberson S. 2023. Data to decisions: how to make science more relevant for management of the San Francisco Estuary. San Franc Estuary Watershed Sci. [accessed 2026 Jun 27];21(1). *https://doi.org/10.15447/sfews.2023v21iss1art1*

Spier C, Stringfellow W, Hanlon J, Brunell M, Estiandan M, Koski T, Kääriä T. 2013. Unprecedented bloom of toxin-producing cyanobacteria in the southern Bay–Delta estuary and its potential negative impact on the aquatic food web. University of the Pacific Ecological Engineering Program Report 4.5.1/DWR 745. [accessed 2026 Jun 27]. 30 p. Available from: *https://www.waterboards.ca.gov/waterrights/water_issues/programs/bay_delta/california_waterfix/exhibits/docs/petitioners_exhibit/CDWR/CDWR-745.pdf*

Sutula M, Kudela R, Hagy JD III, Harding LW Jr, Senn D, Cloern JE, Bricker S, Berg GM, Beck M. 2017. Novel analyses of long-term data provide a scientific basis for chlorophyll-a thresholds in San Francisco Bay. Estuar Coast Shelf Sci. [accessed 2026 Jun 27];197:107–118. *https://doi.org/10.1016/j.ecss.2017.07.009*

Tett P, Gilpin L, Svendsen H, Erlandsson CP, Larsson U, Kratzer S, Fouilland E, Janzen C, Lee J–Y, Grenz C, et al. 2003. Eutrophication and some European waters of restricted exchange. Cont Shelf Res. [accessed 2026 Jun 27];23:1635–1671. *https://doi.org/10.1016/j.csr.2003.06.013*

[US EPA] US Environmental Protection Agency.-2023. HAB Methods. Washington (DC): US EPA, Office of Water. [updated 2026 Aug 25; accessed 2026 Aug 29]. *https://www.epa.gov/habs/hab-methods*

Vareli K, Zarali E, Zacharioudakis GS, Vagenas G, Varelis V, Pilidis G, Briasoulis E, Sainis I. 2012. Microcystin-producing cyanobacterial communities in Amvrakikos Gulf (Mediterranean Sea, NW Greece) and toxin accumulation in mussels (*Mytilus galloprovincialis*). Harmful Algae. [accessed 2026 Jun 27];15:109–118. *https://doi.org/10.1016/j.hal.2011.12.005*

Verspagen JM, Snelder EOFM, Visser PM, Jöhnk KD, Ibelings BW, Mur LR, Huisman J. 2005. Benthic–pelagic coupling in the population dynamics of the harmful cyanobacterium *Microcystis.* Freshw Biol. [accessed 2026 Jun 27];50(5):854–867. *https://doi.org/10.1111/j.1365-2427.2005.01368.x*

Wood SN. 2004. Stable and efficient multiple smoothing parameter estimation for generalized additive models. J Am Stat Assoc. [accessed 2026 Jun 27];99:673–686. *https://doi.org/10.1198/016214504000000980*

Wynne TT, Meredith A, Mishra S, St. Laurent K, Stumpf R. 2026. Processing methods and guidelines for NCCOS harmful algal bloom forecasting satellite products. NOAA Technical Memorandum NOS NCCOS 366. [accessed 2026 Aug 29]. *https://doi.org/10.25923/v03z-gc36*

Xiao M, Li M, Reynolds CS. 2018. Colony formation in the cyanobacterium *Microcystis*. Biol Rev. [accessed 2026 Jun 27];93:1399–1420. *https://doi.org/10.1111/brv.12401*

You J, Mallery K, Hong J, Hondzo M. 2018. Temperature effects on growth and buoyancy of *Microcystis aeruginosa*. J Plankton Res. [accessed 2026 Jun 27];40(1):16–28. *https://doi.org/10.1093/plankt/fbx059*

Zhu L, Zhang H, Guo L, Huang W, Gong W. 2021. Estimation of riverine sediment fate and transport timescales in a wide estuary with multiple sources. J Mar Syst. [accessed 2026 Jun 27];214:103488. *https://doi.org/10.1016/j.jmarsys.2020.103488*

Zuur AF, Ieno EN, Walker NJ, Saveliev AA, Smith GM. 2009. Mixed effects models and extensions in ecology with R. New York (NY): Springer. 574 p.

NOTES

Flynn T. 2025. Phone conversation with E. Preece on Microcystis sampling techniques and Microcystis distribution through the photic zone. West Sacramento, CA.

[CDWR] California Department of Water Resources. 2025. Unpublished data available from Brianne Sakata at brianne.sakata@water.ca.gov.